



## Research paper

# Monoterpenoid-based inhibitors of filoviruses targeting the glycoprotein-mediated entry process

Anastasiya S. Sokolova<sup>a,\*</sup>, Olga I. Yarovaya<sup>a,b</sup>, Anastasiya V. Zybkina<sup>c</sup>, Ekaterina D. Mordvinova<sup>a,c</sup>, Nadezhda S. Shcherbakova<sup>c</sup>, Anna V. Zaykovskaya<sup>c</sup>, Dmitriy S. Baev<sup>a</sup>, Tatyana G. Tolstikova<sup>a,b</sup>, Dmitriy N. Shcherbakov<sup>c</sup>, Oleg V. Pyankov<sup>c</sup>, Rinat A. Maksyutov<sup>c</sup>, Nariman F. Salakhutdinov<sup>a</sup>

<sup>a</sup> N.N.Vorozhtsov Novosibirsk Institute of Organic Chemistry SB RAS, 630090, Novosibirsk, Lavrent'ev Av., 9, Russia

<sup>b</sup> Novosibirsk State University, 630090, Novosibirsk, Pirogova St., 1, Russia

<sup>c</sup> State Research Center of Virology and Biotechnology VECTOR, Rospotrebnadzor, 630559, Koltsovo, Novosibirsk Region, Russia

## ARTICLE INFO

## Article history:

Received 28 May 2020

Received in revised form

21 July 2020

Accepted 3 August 2020

Available online 20 August 2020

## Keywords:

Borneol

Camphor

Ebola virus

Marburg virus

Glycoprotein

Mutagenesis study

## ABSTRACT

In this study, we screened a large library of (+)-camphor and (–)-borneol derivatives to assess their filovirus entry inhibition activities using pseudotype systems. Structure-activity relationship studies revealed several compounds exhibiting submicromolar IC<sub>50</sub> values. These compounds were evaluated for their effect against natural Ebola virus (EBOV) and Marburg virus. Compound **3b** (**As-358**) exhibited the good antiviral potency (IC<sub>50</sub> = 3.7 μM, SI = 118) against Marburg virus, while the hydrochloride salt of this compound **3b-HCl** had a strong inhibitory effect against Ebola virus (IC<sub>50</sub> = 9.1 μM, SI = 31) and good *in vivo* safety (LD<sub>50</sub> > 1000 mg/kg). The results of molecular docking and *in vitro* mutagenesis analyses suggest that the synthesized compounds bind to the active binding site of EBOV glycoprotein similar to the known inhibitor toremifene.

© 2020 Elsevier Masson SAS. All rights reserved.

## 1. Introduction

Filoviruses belong to the *Filoviridae* family and can cause severe hemorrhagic fever in humans and nonhuman primates, with a mortality rate of up to 90%. Two human pathogenic genera of this virus family have been identified: *Ebolavirus* and *Marburgvirus*. The genus *Ebolavirus* has six species, among which the prototypic virus Zaire ebolavirus [now known as Ebola virus (EBOV)], Sudan (SUDV), Bundibugyo (BDBV), Reston (RESTV), Tai Forest (TAFV) and Bombali virus (BOMV). Bombali virus is a new species that was identified in Sierra Leon and Angolan free-tailed bats [1]. The Ebola virus was first identified in 1976 during outbreaks in the Sudan and Congo [2], since which time several outbreaks have occurred. The largest outbreak in West African 2013–16 resulted in more than 28,000 infected cases and over 11,000 deaths. On August 1, 2018, the Ministry of Health of the Democratic Republic of the Congo (DRC)

declared a new outbreak of Ebola virus disease in North Kivu Province. The latest numbers provided by the WHO regarding the Ebola outbreak in DRC as of March 16, 2020 included 3310 confirmed cases and 2264 deaths [3]. Human pathogenic filoviruses are believed to exclusively occur in regions of Africa, although filovirus-specific antibodies have been detected in animals in Singapore [4] and China [5]. The results of these serological studies suggest that filoviruses could also be widely distributed in Asia.

To date, no antiviral therapeutic for Ebola virus infections has been licensed, with treatment primarily focusing on supportive measures. A number of experimental therapies were tested during the latest Ebola virus epidemic, including monoclonal antibodies (ZMapp, mAb 114 and REGN-EB3) and the small-molecule inhibitor remdesivir (GS-5734), although evidence for the efficacy of these therapies is still lacking [6]. Thus, the continuous re-emergence of Ebola virus disease (EVD) outbreaks in Africa coupled with the potential risk of the expansion of epidemics in other continents, as well as the possibility of the use EBOV as bioweapon and a lack of approved therapeutics to treat EVD makes the development of effective anti-EBOV therapeutics one of the top public health

\* Corresponding author.

E-mail address: [asokolova@nioch.nsc.ru](mailto:asokolova@nioch.nsc.ru) (A.S. Sokolova).

priorities.

The RNA genome of EBOV harbors seven genes that encode at least ten proteins: nucleoprotein (NP); viral proteins (VP24, VP30, VP35, and VP40); glycoprotein (GP); soluble GP (sGP); small sGP;  $\Delta$ -peptide; and polymerase (L) [7]. EBOV glycoprotein (EBOV GP) is the key protein that mediates viral entry into host cells and provides a potential target for the discovery anti-EBOV agents, because inhibition of this glycoprotein can block the propagation of the virus at an early stage, minimizing the chance for the virus to evolve. The entry process includes five steps: 1) viral attachment to the cell surface via interactions between GP and host cell receptors; 2) viral uptake into host cells by macropinocytosis; 3) GP cleavage by cathepsins B and L; 4) GP interaction with the host protein Niemann-Pick C1 (NPC1), which is necessary for the virus to bind the endosomal membrane [8]; and 5) the release of viral particles. Each of these steps, as well as the cellular functions associated with these steps, are potential targets for the discovery anti-filovirus agents. Recently, a large number of small-molecule entry inhibitors have been identified, several of them illustrated in Fig. 1 and including inhibitors of cell surface attachment (MLS000534476), macropinocytosis inhibitor (MLS000394177) and lysosomal cysteine cathepsin inhibitors, such as R11P [9,10]. Also an inhibitor of two-pore  $\text{Ca}^{2+}$  channel 2 (TPC2), alkaloid tetrandrine, showed partial protective activity *in vivo* in a lethal mouse model [11].

Several FDA-approved drugs inhibit the EBOV entry process by destabilizing the GP. The most prominent of these compounds include the selective estrogen receptor modulator toremifene (Fig. 1); the painkiller ibuprofen; the antipsychotic drugs benzotropine and thioridazine; and the antidepressants paroxetine and sertraline [12]. High-resolution complexes of GP-toremifene and GP-ibuprofen were obtained and show that they bind in a cavity between the attachment (GP1) and fusion (GP2) subunits (Fig. 2). Thus, targeting the entry process is a rapidly developing strategy for the discovery of antivirals against filoviruses.

Recently, we identified camphor and borneol derivatives as effective inhibitors of influenza virus replication [13–15]. Among these compounds, (+)-1,7,7-trimethylbicyclo[2.2.1]heptan-2-ylidene-aminoethanol (camphene) is one of the most effective [15,16]. Through fusion inhibition assays, camphene was shown to inhibit the surface glycoprotein hemagglutinin (HA) activities of influenza A and B viruses [17]. In addition, we identified heterocyclic derivatives of (–)-borneol as potent inhibitors of influenza A viruses. Similar to filovirus GP, the influenza virus protein HA binds sialic acid on host cells and is responsible for membrane fusion. Moreover, influenza virus and filovirus class I fusion proteins have similar pre- and postfusion forms [18]. Therefore, we screened large

library camphor and borneol derivatives in a Marburg glycoprotein-mediated VSV pseudotype system, which resulted in the identification of N-heterocyclic borneol derivatives that block the entry step of Marburg virus [19]. Compounds **3b** (As-358) and **4b** containing a piperidine and 4-methylpiperidine moieties exhibited the highest virus-specific activities, with  $\text{IC}_{50}$  values of 9 and 4  $\mu\text{M}$ , respectively (Fig. 3). Preliminary structure-activity relationship (SAR) studies revealed that crucial structural fragment included a 1,7,7-trimethylbicyclo[2.2.1]heptan scaffold and heterocyclic ring, such as piperidine, 4-methylpiperidine, 1-methylpiperazine, 1-ethylpiperazine. Moreover, showed that the combination of this saturated N-heterocycle and 1,7,7-trimethylbicyclo[2.2.1]heptan scaffold was favorable for antiviral activity against orthopoxvirus infection [20].

In this study, we expanded our SAR studies of borneol esters with the aim of identifying other potent small molecule filovirus inhibitors (Fig. 4). We synthesized a series of (–)-borneol esters to assess the effects of different N-containing heterocycles as well as the effects of spacer length and the chiral configuration of 1,7,7-trimethylbicyclo[2.2.1]heptan scaffold on filovirus inhibition. A series of (+)-camphor amides were synthesized to evaluate the effect of the replacement of the ester group by an amide on anti-filovirus activity. In addition, we conducted molecular docking and site-directed mutagenesis analyses to identify a possible binding site of the synthesized agents.

## 2. Results

### 2.1. Chemistry

The syntheses of compounds **2-7a-c** and **8a-b** were previously reported [14,20]. Using similar methods, we synthesized compounds **3-4d**, **8c** and **9-14a-c** as illustrated in Scheme 1. Acylation of (–)-borneol with chloroacetyl chloride or the chlorine-containing chloride **1a-c** generated esters **2a-d** with good yields. The desired products were produced from interactions with the key intermediates **2a-d** with the corresponding amines.

Being a nitrogenous compound, salt formation was envisaged as one of the approaches to enhance solubility of synthesized compounds, therefore, HCl salts of compounds **3b** and **4b** (**3b-HCl** and **4b-HCl**) were generated.

To assess the effect of the ester group on antiviral activity, a series of amides containing heterocycles and linkers of different lengths were synthesized. Target amides were generated using commercially available (+)-camphor. The syntheses of amides **18-20a-b** and **21b** were previously reported [20]. The new amides were synthesized using a similar method as depicted in Scheme 2.

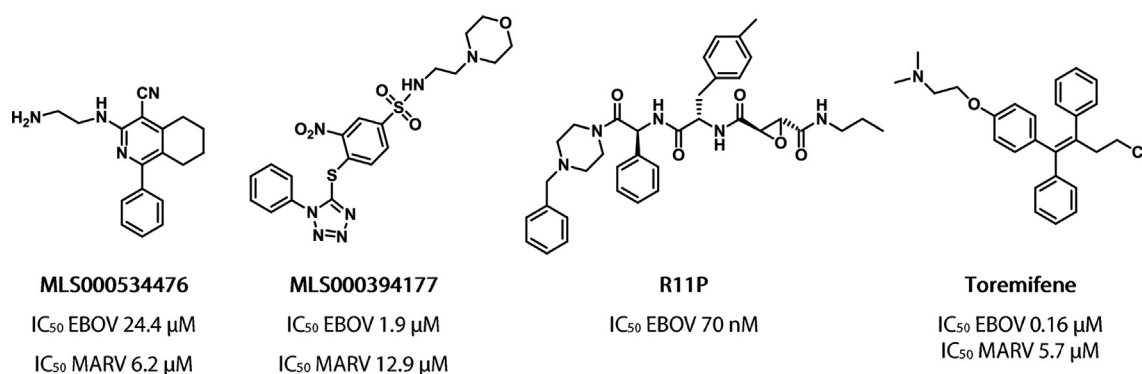
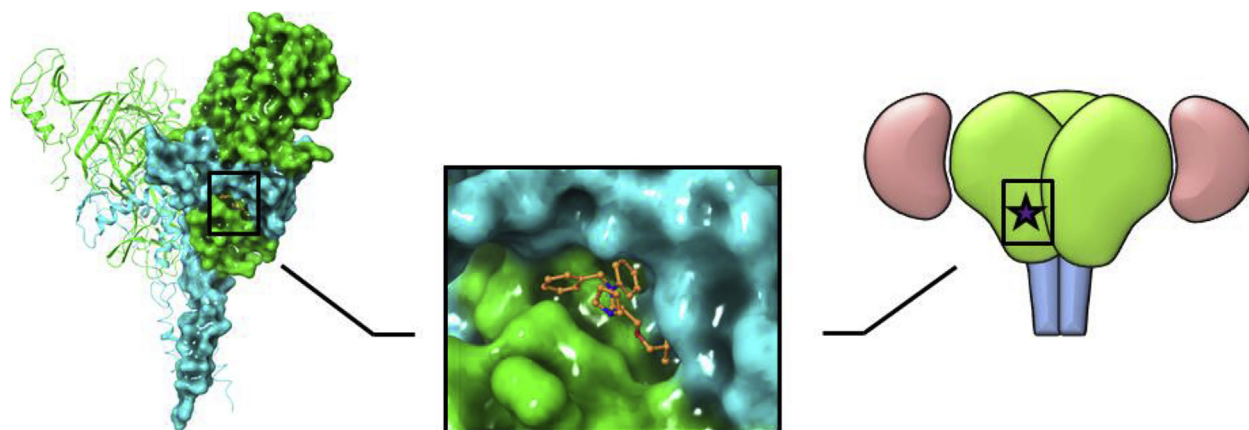
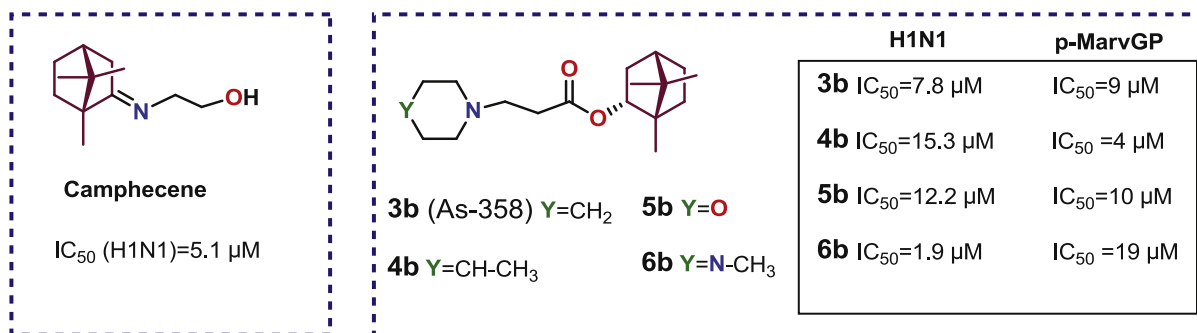


Fig. 1. Compounds inhibiting the filovirus entry process.



**Fig. 2.** Overall structure of EBOV GP-toremifene (left). A schematic representation of the GP-toremifene complex (right), showing GP1 (green), GP2 (blue), and the mucin-like domain (pink). An enlarged fragment of an inhibitor-binding site complex (center). (For interpretation of the references to color in this figure legend, the reader is referred to the Web version of this article.)



**Fig. 3.** Structures of antiviral agents based on (+)-camphor and (-)-borneol.

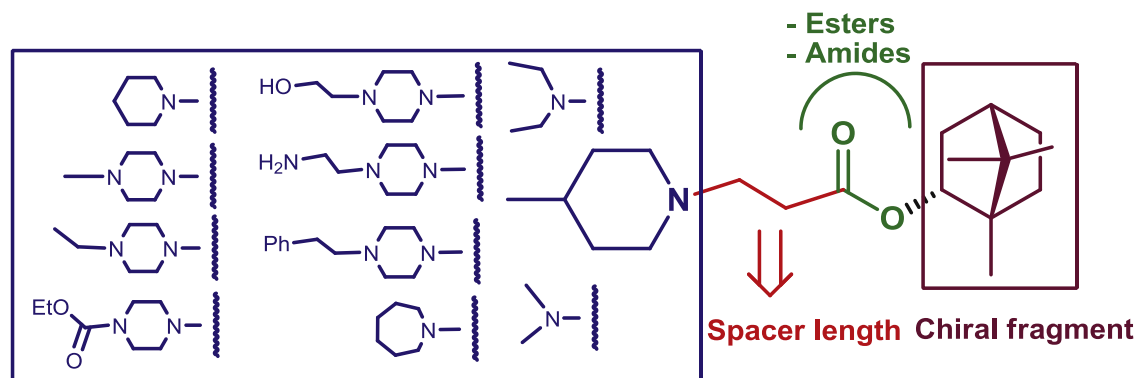
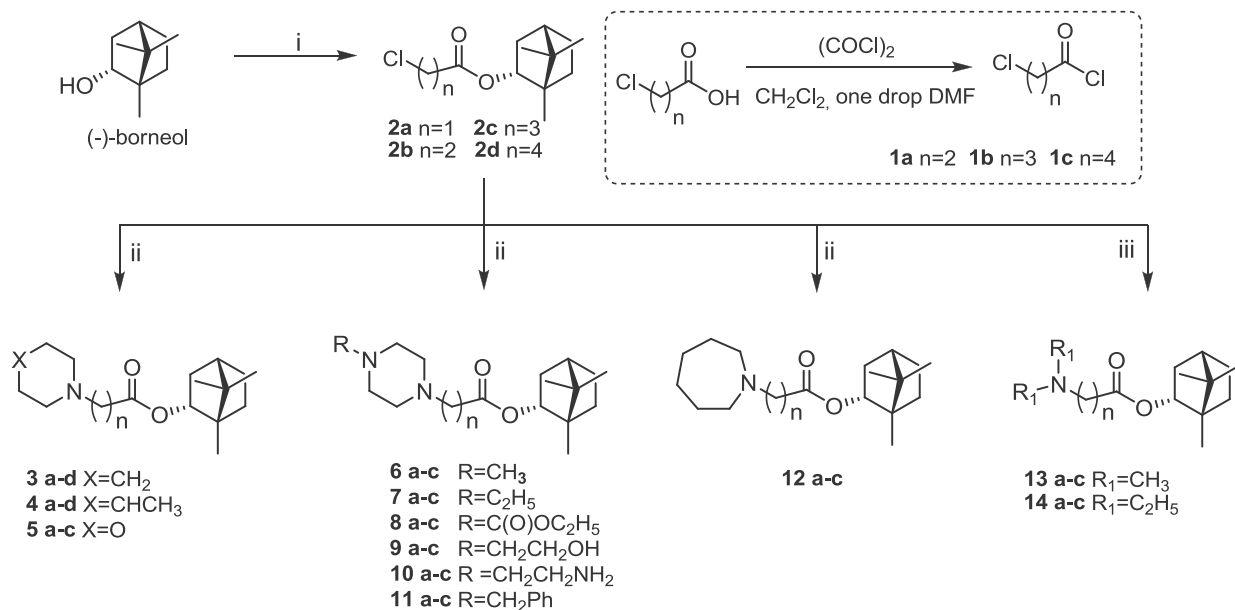


**Fig. 4.** The strategy used for structure-activity relationship studies.

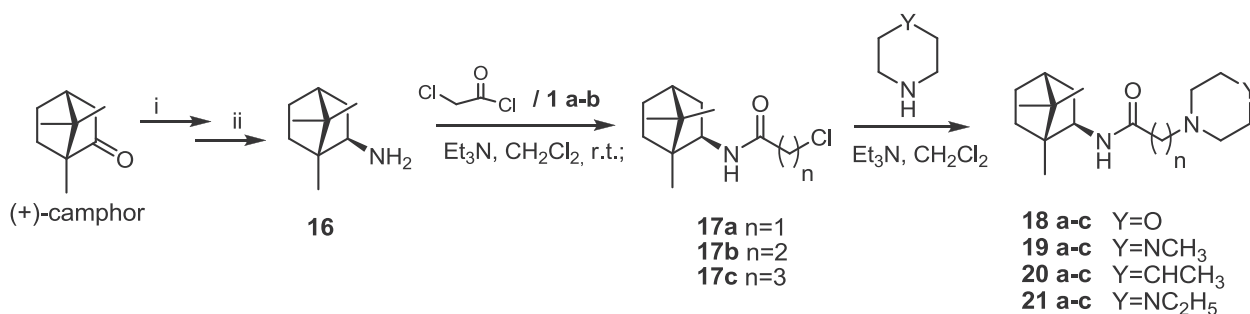
In the first stage, camphor oxime was prepared, and its subsequent reduction with NaBH<sub>4</sub> in the presence of NiCl<sub>2</sub> resulted in the (1R, 2R)-bornyl amine **16**. The reaction between amine **16** and chloroacetyl chloride or the chlorine-containing compounds **1a-b** led to key intermediates **17a-c**. At the final stage, the chlorine-containing amides **17a-c** were reacted with morpholine, 4-methylpiperidine, 1-methylpiperazine or 1-ethylpiperazine to obtain the target substances **18–21a-c**.

To study the effect of the chiral configuration of borneol hydroxy groups on antiviral activity, a group of (+)- and (-)-isoborneol

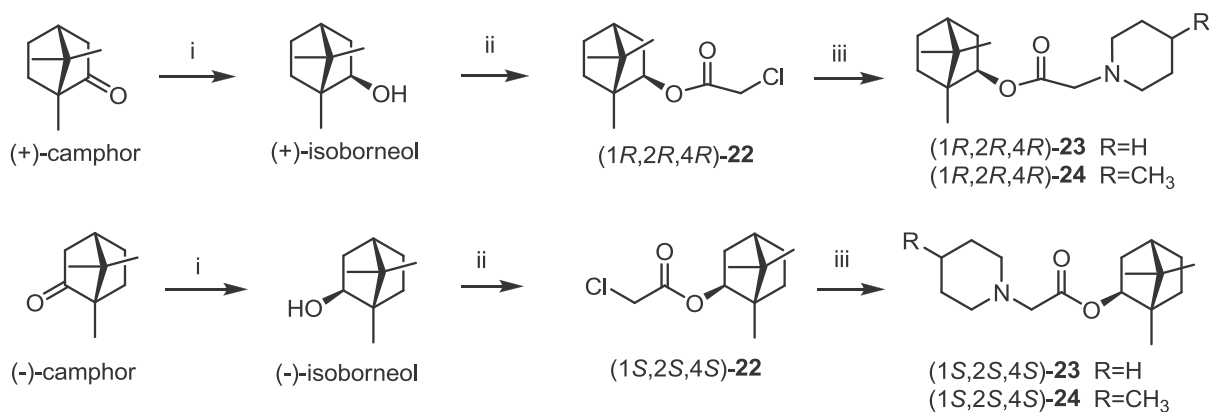
derivatives were generated. The synthesis of two enantiomers of isoborneol derivatives is shown in [Scheme 3](#). (+)-Camphor NaBH<sub>4</sub> was reduced to give a 10:1 exo:endo mixture of isomers [(+)-isoborneol and (+)-borneol, respectively]. Subsequent chromatographic separation led to the desired exo isomer, namely, (+)-isoborneol, and (-)-isoborneol was prepared in a similar manner from commercially available (-)-camphor. From the prepared (+)- and (-)-isoborneols, the target compounds (1R,2R,4R)-**23–24** and (1S,2S,4S)-**23–24** were similarly prepared as shown in [Scheme 1](#).



**Scheme 1.** Reagents and conditions: (i) corresponding chloroacetyl chloride, Et<sub>3</sub>N, CH<sub>2</sub>Cl<sub>2</sub>, r.t.; (ii) the corresponding amine, Et<sub>3</sub>N, CH<sub>2</sub>Cl<sub>2</sub>, r.t.; (iii) diethylamine or triethylamine, K<sub>2</sub>CO<sub>3</sub>, CH<sub>3</sub>CN, r.t.-reflux.



**Scheme 2.** Reagents and conditions: (i) NH<sub>2</sub>OH·HCl, AcONa, and EtOH–H<sub>2</sub>O (8:2), reflux; (ii) NiCl<sub>2</sub>, NaBH<sub>4</sub>, and MeOH, –30 °C.



**Scheme 3.** Reagents and conditions: (i) NaBH<sub>4</sub> and MeOH, –30 °C; (ii) chloroacetyl chloride, Et<sub>3</sub>N, and CH<sub>2</sub>Cl<sub>2</sub>, r.t.; (iii) piperidine or 4-methylpiperidine, Et<sub>3</sub>N, and CH<sub>2</sub>Cl<sub>2</sub>, r.t.

## 2.2. Evaluation of in vitro antiviral activity using pseudotype viruses and SAR study

Considering the high lethality of EBOV and the lack of prophylactic and therapeutic treatments, studies using the authentic virus

can only be performed in laboratories with BSL-4 containment. To overcome this issue, in the first stage, the activity of synthesized compounds was studied using a “surrogate” system, which allowed for entry inhibitors to be identified under BSL-2 containment. This system included vesicular stomatitis virus (VSV) particles

pseudotyped with EBOV GP. The potency against Ebola pseudotype viruses (rVSV- $\Delta$ G-EboV-GP) of all synthesized compounds and cytotoxicity are displayed in Tables 1–3. The sertraline was used as a reference drug, since there are data confirming the efficient binding of this drug to GP EBOV [12]. To determine the specific inhibitory activity of the compounds toward rVSV- $\Delta$ G-EboV-GP, antiviral activities against viral particles pseudotyped G VSV (rVSV- $\Delta$ G-G) were determined. Using this approach, compounds that similarly inhibit both viruses will likely affect cellular mechanisms common to the entry of both viruses.

First, we examined the effect of different heterocyclic or dialkylamino groups and linker lengths on antiviral activity (Table 1). The SAR results showed that a morpholine ring is not favorable for inhibiting activity, although the derivatives **5a-c** displayed low toxicity ( $CC_{50}$  = 210–326  $\mu$ M). The piperidine and 4-methylpiperidine derivatives **3-4b-d**, which had a long linker ( $n \geq 2$ ), displayed potent inhibition efficiency, with high SI values of 162–956. The hydrochloride salts **3b-HCl** and **4b-HCl** showed promising antiviral activity ( $IC_{50}$  = 0.8 and 0.4  $\mu$ M, respectively) but were significantly more toxic ( $CC_{50}$  = 87.0 and 69.8  $\mu$ M, respectively) compared to the free bases **3b** and **4b** ( $CC_{50}$  = 289.7 and 279.7  $\mu$ M, respectively). Almost all of the 4-substituted piperazine derivatives displayed good antiviral potency, with the exception of the ethyl piperazine-1-carboxylate derivatives **8a-c**, which displayed weak inhibition. The derivatives **6-7b-c** and **9b-c**, which harbor alkyl or hydroxyethylene groups in the piperazine ring with linker lengths of  $n \geq 2$ , were significantly more active, exhibiting  $IC_{50}$  values between 0.1 and 1.8  $\mu$ M and  $CC_{50}$  values ranging from 99.2 to 282  $\mu$ M. The piperazine derivative **10c**, containing 2-aminoethyl substitution at the nitrogen atom, showed low  $IC_{50}$  values and high toxicity, while compound **10a** had a  $CC_{50}$  value of 247  $\mu$ M and an SI value of 114. Interestingly, a lipophilic benzyl group at the nitrogen atom significantly increased the toxicity of compounds **11a-c**, which had  $CC_{50}$  values ranging from 30 to 59  $\mu$ M. In addition, the azepane derivatives **12a** and **12c** demonstrated high toxicity, whereas compound **12b**, with linker length of  $n = 2$ , exhibited a high  $CC_{50}$  value of 182  $\mu$ M and moderate activity, with an  $IC_{50}$  value of 5.1  $\mu$ M. Derivatives with N,N-dialkylamine symmetric groups did not show appreciable antiviral activity, with the exception of (1S,2S,4S)-1,7,7-trimethylbicyclo[2.2.1]heptan-2-yl 4-(diethylamino)butanoate (**14c**) displayed high anti-rVSV- $\Delta$ G-EboV-GP activity, with an  $IC_{50}$  value of 0.3  $\mu$ M, and low toxicity ( $CC_{50}$  = 165  $\mu$ M). These results indicated that the piperidine, 4-methylpiperidine, and 4-alkyl or -hydroxyalkyl substituted piperazine ring may be more favorable than morpholine, azepane or 4-benzyl substituted piperazine groups. In this study, we confirmed that linker length greatly affects toxicity. The piperidine, 4-methylpiperidine, N-ethyl piperazine and azepane derivatives were the least toxic, with linker lengths of  $n = 2$ , compared to compounds where  $n = 1$  or 3,4.

Next, we examined the effect of the chiral configuration of the 1,7,7-trimethylbicyclo[2.2.1]heptan moiety on antiviral activity (Table 2). In general, comparing compounds with the same substituents **3-4 a** and (1R,2R,4R)-, (1S,2S,4S)-**23-24**, the (+)- and (-)-isoborneol derivatives (1R,2R,4R)-**23-24** and (1S,2S,4S)-**23-24** showed lower values of  $IC_{50}$  than (-)-borneol derivatives **3a** and **4a**. However, (+)- and (-)-isoborneol derivatives were more toxic than analogues in the (-)-borneol series.

In the (+)-camphor amide series of compounds **18-21a-c**, all examined compounds possessed good to excellent antiviral activities, with  $IC_{50}$  values between 0.6 and 27  $\mu$ M, and five of these compounds had SI values greater than 100 (Table 3). The MTT test results showed an increase in toxicity with increasing linker length for compounds **17-19a-c**, whereas 4-methylpiperidine derivatives exhibited decreased toxicity with increasing linker length.

### 2.3. In vitro antiviral activity against EBOV and MARV

As previously mentioned, we identified compounds **3b** and **4b** as perspective inhibitors of the entry step of Marburg virus. Further analysis of the *in vitro* antiviral activities of these derivatives using rVSV- $\Delta$ G-EboV-GP viruses showed that they also effectively inhibit the entry step of Ebola virus. Thus, agents **3b** and **4b** and their hydrochloride salts **3b-HCl** and **4b-HCl** were assessed for their antiviral activity against the authentic filoviruses EBOV (strain Zaire) and MARV (strain Popp). Anti-EBOV and anti-MARV assays were conducted at SRC VB Vector in a maximum containment facility (BSL-4). EBOV and MARV were obtained from the State Collection of Viral Infections and Rickettsioses Agents of SRC VB Vector.

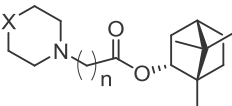
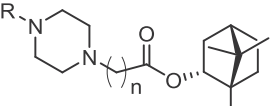
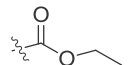
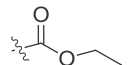
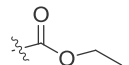
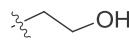
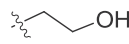
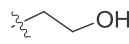
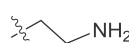
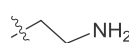
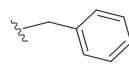
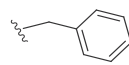
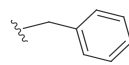
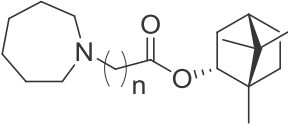
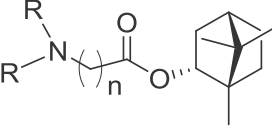
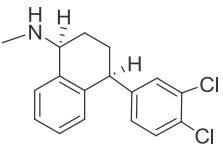
As shown in Table 4, agents **3b**, **4b**, **3b-HCl** and **4b-HCl** were more active against MARV than EBOV. Derivative **3b** was observed to be very potent toward MARV, with micromolar activity ( $IC_{50}$  = 3.7  $\mu$ M) and low toxicity ( $CC_{50}$  = 443  $\mu$ M). In contrast, compound **4b** had a micromolar  $IC_{50}$  value 2.2  $\mu$ M and displayed a higher degree of toxicity ( $CC_{50}$  = 69  $\mu$ M) compared to the agent **3b**. Interestingly, the conversion of compound **4b** into the hydrochloride salt **4b-HCl** led to decreased toxicity ( $CC_{50}$  = 144  $\mu$ M) while retaining the same micromolar  $IC_{50}$  value. The salt **3b-HCl**, which contained a piperidin ring, was the most effective inhibitor of EBOV. Despite the fact that piperazine derivatives **6b** and **7b** showed potency against Ebola pseudotype viruses, antiviral activity against the authentic filoviruses did not confirm. The morpholine derivative **5b** showed low activity in the *p*-EBOV and *p*-MARV assay ( $IC_{50}$  = 8.5 and 10  $\mu$ M, respectively) and was not against the authentic filoviruses. These findings demonstrate that the pseudotyped viruses bearing filovirus glycoproteins are a reasonable predictor of activity against authentic filoviruses.

### 2.4. Molecular docking studies

We performed molecular docking studies of synthesized compounds in the active binding site of known inhibitors using an XP (*extra precision*) docking algorithm implemented in the Glide program (Schrödinger Suite 2016–1). Models (PDB IDs: 6F6S, 6F6N, 6F6I, and 6F5U) representing the envelope glycoprotein of the Ebola virus (Zaire ebolavirus, strain Mayinga-76) were selected in combination with pharmacologically significant inhibitors (resolution of 2.07 Å). Features of spatial orientation and noncovalent interactions of the synthesized ligands were compared with the data obtained for known inhibitors. Toremfifene, sertraline, benzotropine, bepridil, paroxetine were selected as known inhibitors. An analysis of the binding site of EBOV GP with cocrystallized inhibitors revealed the presence of a central hydrophobic region (A), a deep hydrophobic pocket (B), and a hydrophilic groove (C) formed by several charged amino acid residues (Fig. 5A). Known inhibitors are located in the central region by the primary parts of the molecules and possess hydrophobic chains positioned in a deep pocket B. Benzotropine, bepridil, paroxetine, sertraline were characterized by interactions with amino acid residues **517** and **548** in this region. For torimephene, an additional structural feature included the presence of a “tail” containing polar groups interacting with charged residues of the hydrophilic furrow, particularly with residue **522** (Fig. 5B).

The synthesized compounds demonstrate a “hybrid” type of binding, where the hydrophobic 1,7,7-trimethylbicyclo [2.2.1] heptan fragment occupies the central region of the binding site, interacting with leucines 515 and 558, methionine 548, alanine 101, tyrosine 517. An aliphatic tail with a nitrogen-containing heterocycle is located in a hydrophilic groove, forming electrostatic interactions with Glu 100 and Asp522 (Fig. 6).

**Table 1**  
Antiviral activities of the synthesized (–)-borneol derivatives.

Compound	n	X/R	CC <sub>50</sub> (μM) <sup>a</sup>	IC <sub>50</sub> (μM)		SIEboV-GP <sup>d</sup>	Ebind <sup>e</sup>
				EboV-GP <sup>b</sup>	VSV-G <sup>c</sup>		
							
<b>3a</b>	n = 1	CH <sub>2</sub>	141.4 ± 14.1	15.7 ± 0.8	122.5 ± 13.5	9	-3.65
<b>3b</b>	n = 2	CH <sub>2</sub>	289.7 ± 22.6	1.7 ± 0.1	93.0 ± 9.3	170	-4.14
<b>3c</b>	n = 3	CH <sub>2</sub>	74.8 ± 6.1	0.3 ± 0.01	50.1 ± 4.5	230	-3.63
<b>3d</b>	n = 4	CH <sub>2</sub>	100.9 ± 12.1	0.6 ± 0.05	105.4 ± 8.4	162	-4.48
<b>3b-HCl</b>	n = 2	CH <sub>2</sub>	87.0 ± 7.8	0.8 ± 0.06	89.4 ± 6.3	112	-4.14
<b>4a</b>	n = 1	CHCH <sub>3</sub>	71.6 ± 6.4	8.5 ± 1.1	35.0 ± 2.4	8	-3.43
<b>4b</b>	n = 2	CHCH <sub>3</sub>	279.7 ± 28.3	0.3 ± 0.04	289.7 ± 19.7	956	-3.80
<b>4c</b>	n = 3	CHCH <sub>3</sub>	171.1 ± 12.8	9.3 ± 1.1	276.4 ± 13.5	18	-4.02
<b>4d</b>	n = 4	CHCH <sub>3</sub>	73.0 ± 3.1	0.2 ± 0.02	83.5 ± 7.3	408	-4.70
<b>4b-HCl</b>	n = 2	CHCH <sub>3</sub>	69.8 ± 5.6	0.4 ± 0.03	71.5 ± 5.4	171	-3.80
<b>5a</b>	n = 1	O	326.9 ± 45.8	24.9 ± 1.1	290.7 ± 26.5	13	-3.07
<b>5b</b>	n = 2	O	304.7 ± 19.5	8.5 ± 0.7	319.8 ± 30.1	36	-4.28
<b>5c</b>	n = 3	O	210.1 ± 14.3	6.5 ± 0.5	287.7 ± 14.4	33	-4.49
							
<b>6a</b>	n = 1	CH <sub>3</sub>	312.5 ± 30.6	6.8 ± 0.8	484.7 ± 48.0	46	-3.53
<b>6b</b>	n = 2	CH <sub>3</sub>	282.0 ± 25.7	0.3 ± 0.03	173.2 ± 15.7	870	-4.89
<b>6c</b>	n = 3	CH <sub>3</sub>	99.2 ± 8.8	0.6 ± 0.04	97.3 ± 8.7	160	-5.00
<b>7a</b>	n = 1	C <sub>2</sub> H <sub>5</sub>	129.7 ± 11.5	1.6 ± 0.1	263.6 ± 21.9	80	-3.30
<b>7b</b>	n = 2	C <sub>2</sub> H <sub>5</sub>	263.6 ± 24.3	1.6 ± 0.1	80.5 ± 5.9	170	-4.85
<b>7c</b>	n = 3	C <sub>2</sub> H <sub>5</sub>	130.8 ± 10.5	0.1 ± 0.01	165.3 ± 11.4	880	-4.77
<b>8a</b>	n = 1		227.0 ± 13.6	19.9 ± 2.1	112.9 ± 8.9	11	-3.70
<b>8b</b>	n = 2		109.7 ± 9.5	28.3 ± 1.9	NT	4	-3.99
<b>8c</b>	n = 3		60.4 ± 4.7	2.6 ± 0.2	49.1 ± 3.8	23	-4.83
<b>9a</b>	n = 1		295.9 ± 32.8	13.9 ± 1.0	394.2 ± 38.2	21	-4.94
<b>9b</b>	n = 2		271.8 ± 32.6	1.8 ± 0.1	258.9 ± 25.9	153	-5.33
<b>9c</b>	n = 3		224.1 ± 28.0	0.3 ± 0.02	192.0 ± 19.2	658	-6.07
<b>10a</b>	n = 1		247.3 ± 23.0	2.2 ± 0.2	24.1 ± 2.4	114	-5.51
<b>10c</b>	n = 3		71.1 ± 5.7	0.6 ± 0.1	50.4 ± 5.1	125	-6.77
<b>11a</b>	n = 1		59.4 ± 5.6	1.3 ± 0.1	39.8 ± 3.4	44	-3.20
<b>11b</b>	n = 2		39.0 ± 3.7	0.3 ± 0.03	27.0 ± 2.4	150	-4.69
<b>11c</b>	n = 3		30.1 ± 2.0	0.3 ± 0.03	26.0 ± 2.3	100	-5.83
							
<b>12a</b>	n = 1		71.6 ± 7.9	1.0 ± 0.1	NT	70	-3.01
<b>12b</b>	n = 2		182.5 ± 16.2	5.1 ± 0.4	191.2 ± 11.1	36	-2.99
<b>12c</b>	n = 3		62.2 ± 5.7	0.2 ± 0.02	NT	250	-4.21
							
<b>13a</b>	n = 1	CH <sub>3</sub>	388.6 ± 38.1	250.7 ± 22.3	522.6 ± 63.2	2	-3.58
<b>13b</b>	n = 2	CH <sub>3</sub>	505.2 ± 34.9	30.0 ± 2.6	NT	17	-3.21
<b>13c</b>	n = 3	CH <sub>3</sub>	100.6 ± 7.0	1.5 ± 0.1	NT	67	-3.53
<b>14a</b>	n = 1	C <sub>2</sub> H <sub>5</sub>	344.0 ± 33.0	5.6 ± 0.5	560.9 ± 66.7	61	-3.09
<b>14b</b>	n = 2	C <sub>2</sub> H <sub>5</sub>	326.9 ± 31.7	12.4 ± 1.1	411.4 ± 48.9	26	-2.55
<b>14c</b>	n = 3	C <sub>2</sub> H <sub>5</sub>	165.8 ± 12.8	0.3 ± 0.03	195.4 ± 23.1	490	-3.05
<b>Sertraline</b>			408 ± 35.9	0.7 ± 0.07	NT	582	-8.24
							

The data represent the mean  $\pm$  SD from three independent experiments.

NT not tested.

<sup>a</sup> CC<sub>50</sub>: the median cytotoxic dose, i.e. the concentration causing 50% cell death.

<sup>b</sup> IC<sub>50</sub> (EboV-GP): the concentration of a compound required to inhibit rVSV-ΔG-EboV-GP infection of HEK293T cells by 50%.

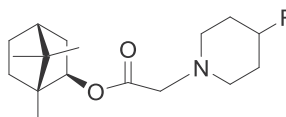
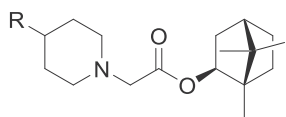
<sup>c</sup> IC<sub>50</sub> (VSV-G): the concentration of a compound required to inhibit rVSV-ΔG-G infection of HEK293T cells by 50%.

<sup>d</sup> S<sub>EboV-GP</sub> = CC<sub>50</sub>/IC<sub>50</sub> (EboV-GP).

<sup>e</sup> E<sub>bind</sub>: binding energy, kcal/mol (the value is not genuine binding energy but rather an estimated docking score).

**Table 2**

Antiviral activities of the (+)- and (-)-isborneol derivatives against rVSV-ΔG-EboV-GP virus.

Compound	R	CC <sub>50</sub> (μM) <sup>a</sup>	IC <sub>50</sub> EboV-GP <sup>b</sup>	SI <sup>c</sup>	E <sub>bind</sub> <sup>d</sup>
					
(1R,2R,4R)- <b>23</b>	H	80.5 $\pm$ 9.9	2.9 $\pm$ 0.3	28	-3.99
(1R,2R,4R)- <b>24</b>	CH <sub>3</sub>	34.1 $\pm$ 4.0	3.1 $\pm$ 0.3	11	-4.36
					
(1S,2S,4S)- <b>23</b>	H	89.5 $\pm$ 8.0	3.6 $\pm$ 0.3	25	-3.72
(1S,2S,4S)- <b>24</b>	CH <sub>3</sub>	34.1 $\pm$ 2.7	4.4 $\pm$ 0.4	8	-4.36

<sup>a</sup> CC<sub>50</sub>: the median cytotoxic dose, i.e. the concentration causing 50% cell death.

<sup>b</sup> IC<sub>50</sub> EboV-GP: the concentration of a compound required to inhibit rVSV-ΔG-EboV-GP infection of HEK293T cells by 50%, μM.

<sup>c</sup> S<sub>EboV-GP</sub> = CC<sub>50</sub>/IC<sub>50</sub> (EboV-GP).

<sup>d</sup> E<sub>bind</sub>: binding energy, kcal/mol (the value is not genuine binding energy but rather an estimated docking score).

## 2.5. Site-directed mutagenesis

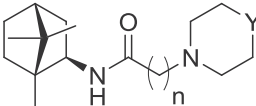
Based on the molecular docking results we made 3 rVSV pseudotyped with mutant GP proteins carrying single alanine substitutions at the **517**, **522** and **548** amino acids positions of chain B of

the GP2 subunit. The antiviral activity of the mutated EboV-GP particles was compared with the wild-type WT-EboV-GP. The mutant pseudotyped VSV particles were tested against the following selected compounds: **4b**, **3b** and **7b**, which were tested on natural filovirus; **4c** and **6c**, with long linkers; and two (+)-camphor amides, **18c** and **21a**.

In the antiviral assay, the IC<sub>50</sub> values of agent **3b** toward Y517A-EboV-GP and M548A-EboV-GP were 3.7 and 47.1 μM, respectively (Table 5). A 20-fold increase in the IC<sub>50</sub> value for M548A-EboV-GP was compared to that of the WT-EboV-GP was observed. In contrast, a similar ability of **3b** to inhibit WT-EboV-GP and mutant D522A-EboV-GP was observed (IC<sub>50</sub> 1.7 and 2.2 μM respectively). Similar results were observed for compound **4b**, where a greater than 30-fold increase in the IC<sub>50</sub> value for M548A-EboV-GP was detected compared to that observed for WT-EboV-GP. The inhibitory activity of derivatives **4c** and **6c** toward all mutant pseudotyped viral particles and WT-EboV-GP were different. For agent **4c**, a greater than 20-fold decrease in the IC<sub>50</sub> value toward the mutant Y517A-EboV-GP and D522A-EboV-GP pseudotyped viral particles (IC<sub>50</sub> 0.4 μM) was measured compared to that observed for WT-EboV-GP (IC<sub>50</sub> 9.3 μM). For the derivative **6c**, a greater than 20-fold increase in the IC<sub>50</sub> value was noted for all mutant pseudotyped viral particles compared with that observed for WT-EboV-GP. The inhibitory activities of agent **7b** toward the mutant pseudotyped viral particles were slightly different from the antiviral activity against WT-EboV-GP. The IC<sub>50</sub> values of amide **18b** against WT-EboV-GP and mutant D522A-EboV-GP were almost the same (IC<sub>50</sub> 22.1 and 17.7 μM, respectively), while the IC<sub>50</sub> values against WT-EboV-GP and mutants Y517A-EboV-GP, M548A-EboV-GP significantly different. For the derivative **21a** there is a significant difference was only observed for the mutation Y517A.

**Table 3**

Antiviral activities of the (+)-camphor amides.

Compound	n	Y	CC <sub>50</sub> (μM) <sup>a</sup>	IC <sub>50</sub> (μM)		S <sub>EboV-GP</sub> <sup>d</sup>	E <sub>bind</sub> <sup>e</sup>
				EboV-GP <sup>b</sup>	VSV-G <sup>c</sup>		
							
<b>18a</b>	n = 1	O	838.1 $\pm$ 71.2	5.7 $\pm$ 0.7	838.1 $\pm$ 74.6	147	-3.95
<b>18b</b>	n = 2	O	312.5 $\pm$ 37.8	22.1 $\pm$ 2.2	312.5 $\pm$ 21.9	14	-3.61
<b>18c</b>	n = 3	O	171.8 $\pm$ 21.1	9.4 $\pm$ 0.7	171.8 $\pm$ 10.3	18	-4.76
<b>19a</b>	n = 1	N-CH <sub>3</sub>	853.3 $\pm$ 101.5	13.3 $\pm$ 1.1	853.3 $\pm$ 42.7	64	-3.81
<b>19b</b>	n = 2	N-CH <sub>3</sub>	485.6 $\pm$ 55.4	2.6 $\pm$ 0.3	485.6 $\pm$ 19.4	187	-5.89
<b>19c</b>	n = 3	N-CH <sub>3</sub>	474.7 $\pm$ 51.7	2.5 $\pm$ 0.3	474.7 $\pm$ 21.4	191	-5.29
<b>20a</b>	n = 1	N-C <sub>2</sub> H <sub>5</sub>	660.2 $\pm$ 71.3	8.5 $\pm$ 0.8	660.2 $\pm$ 30.4	78	-4.67
<b>20b</b>	n = 2	N-C <sub>2</sub> H <sub>5</sub>	564.9 $\pm$ 49.7	0.6 $\pm$ 0.04	564.9 $\pm$ 49.7	908	-5.15
<b>20c</b>	n = 3	N-C <sub>2</sub> H <sub>5</sub>	268.2 $\pm$ 17.9	2.1 $\pm$ 0.14	268.2 $\pm$ 23.6	129	-5.76
<b>21a</b>	n = 1	CHCH <sub>3</sub>	78.0 $\pm$ 6.9	27.0 $\pm$ 1.6	78.0 $\pm$ 6.9	2.9	-4.65
<b>21b</b>	n = 2	CHCH <sub>3</sub>	93.6 $\pm$ 10.0	2.6 $\pm$ 0.1	93.6 $\pm$ 7.3	36	-3.70
<b>21c</b>	n = 3	CHCH <sub>3</sub>	141.6 $\pm$ 14.3	3.4 $\pm$ 0.3	141.6 $\pm$ 12.7	41	-4.56

<sup>a</sup> CC<sub>50</sub>: the median cytotoxic dose, i.e. the concentration causing 50% cell death.

<sup>b</sup> IC<sub>50</sub> (EboV-GP): the concentration of a compound required to inhibit rVSV-ΔG-EboV-GP infection of HEK293T cells by 50%.

<sup>c</sup> IC<sub>50</sub> (VSV-G): the concentration of a compound required to inhibit rVSV-ΔG-G infection of HEK293T cells by 50%.

<sup>d</sup> S<sub>EboV-GP</sub> = CC<sub>50</sub>/IC<sub>50</sub> (EboV-GP).

<sup>e</sup> E<sub>bind</sub>: binding energy, kcal/mol (the value is not genuine binding energy but rather an estimated docking score).

**Table 4**  
Inhibitory activities of synthesized derivatives against EBOV and MARV.

Compound	CC <sub>50</sub> (μM) <sup>a</sup>	IC <sub>50</sub> (μM) <sup>b</sup> MARV	SI MARV <sup>c</sup>	IC <sub>50</sub> (μM) <sup>d</sup> EBOV	SI EBOV <sup>e</sup>
<b>3b</b>	442.9 ± 82.9	3.7 ± 1.7	118	47.5 ± 8.2	9
<b>3b-HCl</b>	279.1 ± 38.7	18.1 ± 9.3	15	9.1 ± 2.1	31
<b>4b</b>	69.3 ± 5.2	2.2 ± 1.4	32	54.3 ± 14.8	1.3
<b>4b-HCl</b>	144.0 ± 33.2	5.7 ± 3.4	25	64.7 ± 11.2	2.2
<b>5b</b>	122.0 ± 25.6	NA		NA	
<b>6b</b>	61.4 ± 38.5	NA		NA	
<b>7b</b>	19.2 ± 11.8	17.8 ± 4.1	1	NA	
Sertraline <sup>f</sup>		2.43 ± 0.14		3.73 ± 0.62	

NA: not active.

The data represent the mean ± SD from three independent experiments.

<sup>a</sup> CC<sub>50</sub>: 50% cytotoxic concentration (Vero cells).

<sup>b</sup> IC<sub>50</sub>: the concentration of a compound required to inhibit MARV (strain Popp) infection of Vero cells by 50%.

<sup>c</sup> SI MARV: is the selectivity index, which is the CC<sub>50</sub>/IC<sub>50</sub> MARV ratio.

<sup>d</sup> IC<sub>50</sub>: the concentration of a compound required to inhibit EBOV (strain Zaire) infection of Vero cells by 50%.

<sup>e</sup> SI EBOV: is the CC<sub>50</sub>/IC<sub>50</sub> EBOV ratio.

<sup>f</sup> IC<sub>50</sub> values (Vero E6 cells) are taken from Johansen et al. [21].

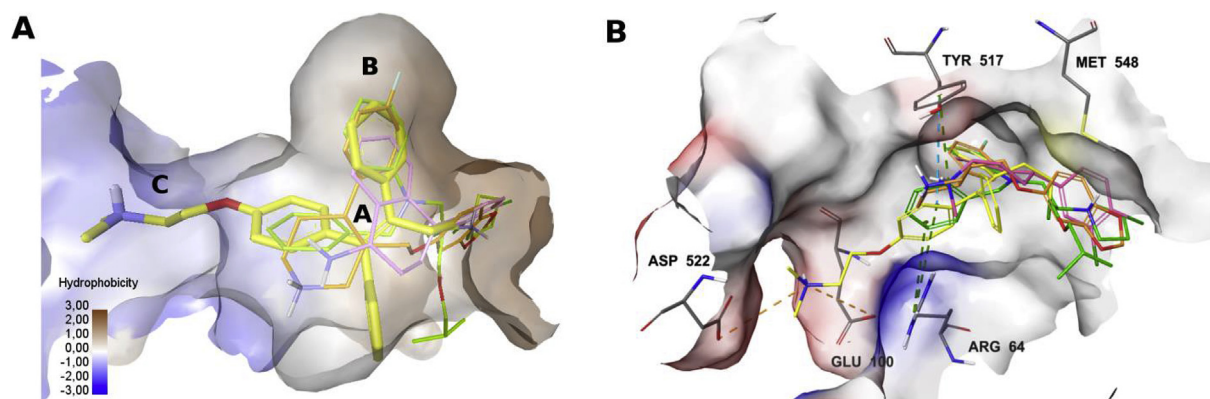


**Fig. 5.** A: The inhibitor binding site pockets. B: Superposition the of pharmacologically significant inhibitors in binding site of EBOV GP. Toremfene, paroxetine, sertraline and bepridil are shown as yellow, orange, pink and green, respectively. (For interpretation of the references to color in this figure legend, the reader is referred to the Web version of this article.)

## 2.6. Acute toxicity studies

The safety of the most active compound (**3b-HCl**) against EBOV was evaluated in outbred ICR mice. Groups of mice were administered either a single dose (1.08, 0.44, 0.27, and 0.14 g/kg) or the vehicle control by gavage in the form of a suspension. The survival of the mice was monitored and recorded over 7 days. No animal deaths were recorded during in the (**3b-HCl**)-treated mice over the entire observation period. Thus, the results of this study indicated that compound (**3b-HCl**) is not toxic to adult mice with intragastric administration ( $LD_{50} > 1000$  mg/kg).

## 3. Discussion

In this study, we describe the preparation and antiviral activities of N-heterocyclic monoterpene derivatives containing an 1,7,7-trimethylbicyclo[2.2.1]heptan scaffold. All synthesized compounds were screened in a cell-based assay for their anti-EBOV activity using a VSV pseudotype by GP EBOV. Almost all of the synthesized compounds showed inhibitory potency against rVSV-ΔG-EboV-GP, ranging from the micromolar range ( $IC_{50} = 30$  μM) to nanomolar range ( $IC_{50} = 0.1$  μM). Moreover, 36 compounds were identified as having low cytotoxicity ( $CC_{50} > 100$  μM) and high selectivity index values. The *in vitro* study results against bona fide EBOV and MARV for the most promising derivatives (**3b**, **3b-HCl**, **4b** and **4b-HCl**) demonstrated their excellent to moderate antiviral

activity. Notably, the most promising anti-EBOV agent (**3b-HCl**) demonstrated good *in vivo* safety. In addition, the *in silico* absorption, distribution, metabolism and excretion (ADME) study results for compounds **3-7b**, **9b-c**, **18b** and **20b** are shown in Table 1S. The calculated parameters are in good agreement with the Lipinski [22] and Ghose [23] rules. For all new compounds, logP does not exceed 5, which indicates good lipophilicity. The most active compounds are characterized by a large scatter of logP values in the range 1.3–4.7. An increase in the linker length directly affects the increase in the logP value in the series of compounds that are identical in structure of the substituent (See SI).

Considering that the synthesized derivatives selectively inhibited rVSV-ΔG-EboV-GP but did not show activity against VSV-G indicate that the likely target of these compounds is GP EBOV. The viral glycoprotein GP consists of two subunits, the receptor attachment glycoprotein 1 (GP<sub>1</sub>) and membrane fusion glycoprotein 2 (GP<sub>2</sub>). GP<sub>1</sub> is responsible for cell surface recognition/attachment and viral uptake into host cells, containing two exterior domains that are responsible for host cell binding and a receptor binding domain (RBD) that interacts with endosomal receptor Niemann-Pick C1 (NPC1). GP<sub>2</sub> is a class I viral fusion protein that catalyzes the fusion of the virus with the host membrane. Previously, a large number of Food and Drug Administration (FDA)-approved drugs were shown to be active against Ebola virus infection. It was shown the anticancer drug toremifene and the painkiller ibuprofen bind in a cavity between the attachment (GP<sub>1</sub>)

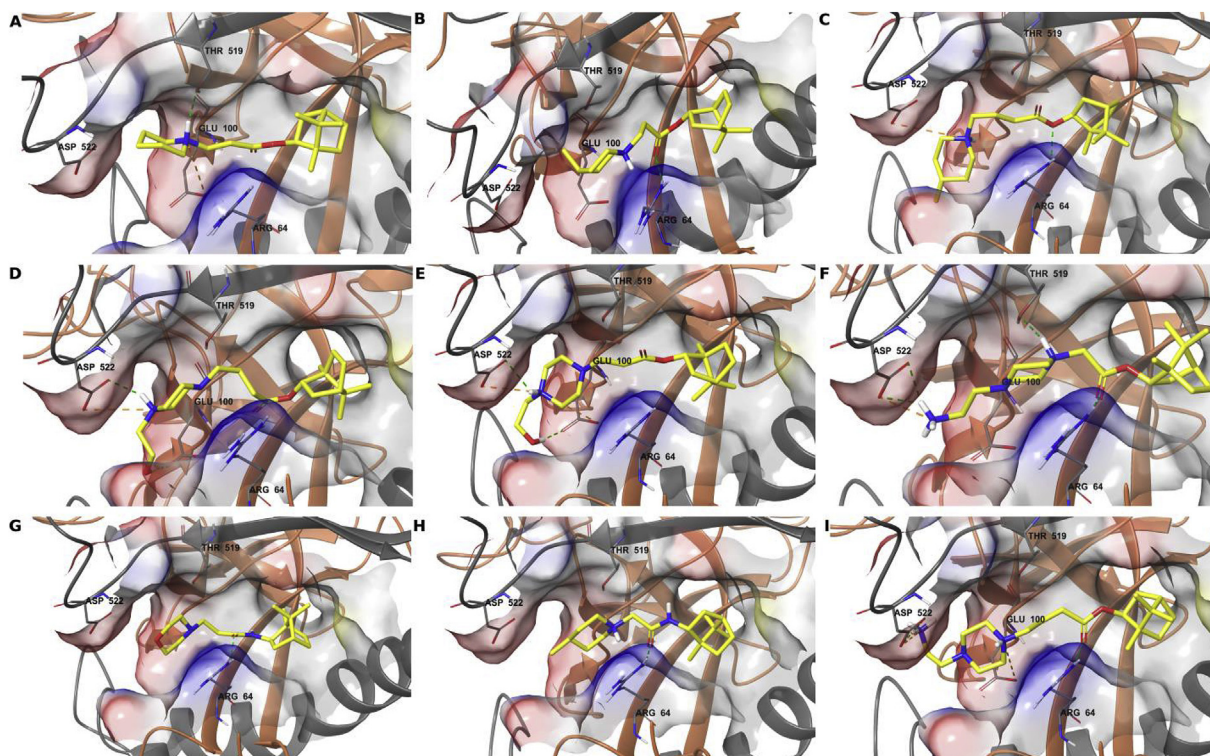


**Fig. 6.** Noncovalent interactions of synthesized agents with amino acid residues of the binding site GP EBOV. **3b** (A); **4b** (B); **4c** (C); **9c** (D); **9b** (E); **10a** (F); **18b** (G); **21a** (H); **10c** (I). Interactions are shown by dashed lines (green, hydrogen bonds; orange, electrostatic interactions), while hydrophobic interactions are not indicated. (For interpretation of the references to color in this figure legend, the reader is referred to the Web version of this article.)

**Table 5**

*In vitro* alanine mutagenesis of the EboV-GP residues Y517, D522 and M548.

Compound	IC <sub>50</sub> (μM)			
	WT-EboV-GP <sup>a</sup>	Y517A-EboV-GP <sup>b</sup>	D522A-EboV-GP <sup>c</sup>	M548A-EboV-GP <sup>d</sup>
<b>3b</b>	1.7 ± 0.2	3.7 ± 0.4	2.2 ± 0.3	47.1 ± 6.1
<b>4b</b>	0.3 ± 0.03	48.1 ± 4.8	4.9 ± 0.5	112.2 ± 14.7
<b>4c</b>	9.3 ± 0.8	0.4 ± 0.03	0.4 ± 0.04	1.2 ± 0.2
<b>6c</b>	0.6 ± 0.1	18.3 ± 2.2	18.3 ± 1.9	12.2 ± 1.4
<b>7b</b>	1.6 ± 0.2	1.8 ± 0.1	0.5 ± 0.04	1.0 ± 0.1
<b>18b</b>	22.1 ± 2.7	173.1 ± 11.8	17.7 ± 1.4	65.2 ± 5.8
<b>21a</b>	27.0 ± 1.9	1.7 ± 0.2	11.6 ± 0.8	44.2 ± 3.4

<sup>a</sup> IC<sub>50</sub> (WT-EboV-GP): the concentration of a compound required to inhibit rVSV-ΔG-EboV-GP infection by 50%.

<sup>b</sup> IC<sub>50</sub> (Y517A-EboV-GP): the concentration of a compound required to inhibit rVSV-ΔG-H517A-EboV-GP infection by 50%.

<sup>c</sup> IC<sub>50</sub> (D522A-EboV-GP): the concentration of a compound required to inhibit rVSV-ΔG-D522A-EboV-GP infection by 50%.

<sup>d</sup> IC<sub>50</sub> (M548A-EboV-GP): the concentration of a compound required to inhibit rVSV-ΔG-M548A-EboV-GP infection by 50%.

and fusion (GP<sub>2</sub>) subunits at the entrance to a large tunnel that links with equivalent tunnels from the other monomers of the trimer at the 3-fold axis. These drugs belong to various pharmacological groups and have different chemical structures but bind in the same cavity on the EBOV GP. Therefore, we performed molecular docking analyses of synthesized compounds in the active binding site of known inhibitors, such as benzotropine, bepridil, paroxetine, sertraline (Figs. 6 and 7).

The *in silico* docking results of synthesized ligands in the binding site EBOV GP (i.e., calculated  $E_{bind}$ ) provided a structural basis to interpret the experimental *in vitro* data. The derivatives **9b**, **9c**, **10a** and **10c** with hydroxyl or amino groups display high antiviral activity against rVSV-ΔG-EboV-GP and exhibited high affinities in *in silico* simulations. This result can be explained by additional interactions between the functional groups of ligands with the amino acid Asp522. Notably, the binding mode of compound **9b** has an

additional hydrogen bond through a hydroxyl group with the charged residue Glu100 (Fig. 6). Glu100 and Thr519 also participate in the interaction with charged nitrogen in the piperidine or piperazine rings, which is probably one of the reasons why the hydrochloride salt **3b-HCl** more active against EBOV than the free base **3b**. Overall, the binding interaction mode of a synthesized ligand with EBOV GP could identify key amino acids, including Glu100, Asp522, Tyr 517, Leu 515, and Met 548, which are important for the of binding in the active site. These results suggest that the synthesized compounds bind EBOV GP similarly to toremifene.

To validate these results, we performed an *in vitro* mutagenesis study of the glycoprotein residues involved in the binding site. To this end, the amino acids M548A, Y517A (two key residues responsible for hydrophobic interaction of all tested compounds) and D522A were all mutated to alanine. Then, the affinities of the rVSV-ΔG-EboV-GP mutants toward compounds **3b**, **4b-c**, **6c**, **7b**,

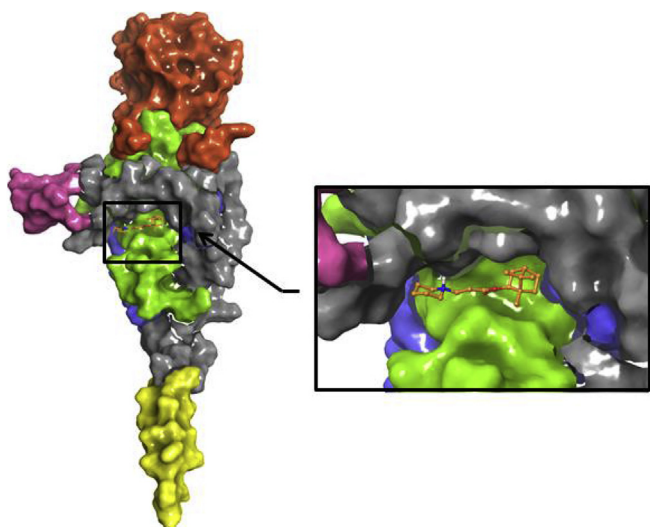


**Fig. 7.** *In silico* docking results of compound **3b**. Regions of EBOV GP are marked by color: receptor binding domain (RBD), green; glycan cap, red; fusion peptide, rose; N-terminal heptad repeat (NHR), blue; and C-terminal heptad repeat (CHR), yellow. (For interpretation of the references to color in this figure legend, the reader is referred to the Web version of this article.)

**18c** and **20a** were evaluated *in vitro* (Table 5). As shown in Table 5, agent **4b** exhibited a greater change in  $IC_{50}$  values for mutants carrying mutations at positions 517 and 548 than at position 522 compared with that observed for the wild-type viral particles. These results agree with those of the molecular docking studies, where for agent **4b**, there is no contact with 522, while this ligand has interactions with Y517 and M548 (Fig. 5). Moreover, the results of the molecular docking and mutagenesis analyses explain the dependence of antiviral activity on the length of the aliphatic “tail”, which is probably due to the necessary length for the interaction of the nitrogen atom with amino acid residue 522. An *in vitro* study using mutant pseudotyped VSV particles of agents **4c** and **6c** also confirmed this hypothesis. As shown in Table 5, these agents demonstrated considerable changes in  $IC_{50}$  values in inhibiting the **Y517A**-EboV-GP, **M548A**-EboV-GP and **D522A**-EboV-GP virus particles. Thus, an increase in the linker length from two methylene

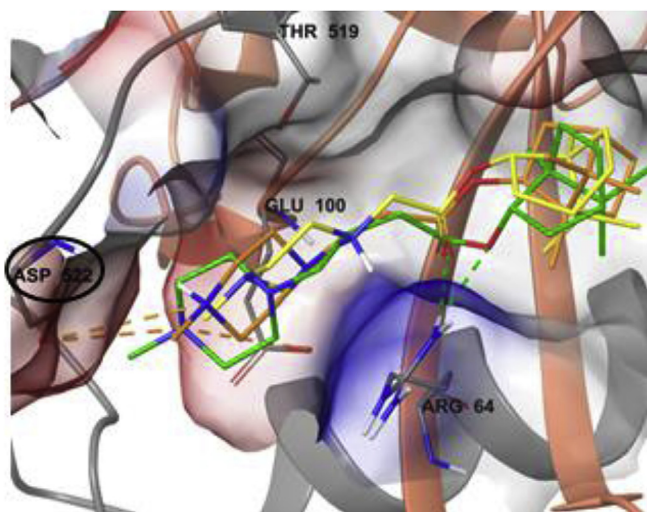


**Fig. 8.** Superposition of the (–)-borneol derivatives **6a**, **6b** and **6c** are shown as yellow, orange and green, respectively. (For interpretation of the references to color in this figure legend, the reader is referred to the Web version of this article.)

groups to three makes it possible for the agents to interact with amino acid D522. As shown in Fig. 8, in contrast to derivative **6b** and **6c** ( $n = 2, 3$ ), derivative **6a** ( $n = 1$ ) had no contacts with residue 522 and showed the lowest antiviral activity ( $IC_{50}^{EboV-GP} = 6.8 \mu M$ ) compared to **6b-c** ( $IC_{50}^{EboV-GP} = 0.3$  and  $0.6 \mu M$ , respectively). In general, for (–)-borneol derivatives, both the computational and *in vitro* experimental results indicated that an increase in the aliphatic carbon chain length ( $n = 1-3$ ) increased the antiviral potency (Table 1).

(+)-Camphor-based amides are probably located in the binding site as shown above. As depicted in Table 5, for agents **18b** and **21a**, the greatest  $IC_{50}$  value change was observed for mutants **Y517A**-EboV-GP and **M548A**-EboV-GP, which was consistent with the *in silico* trend, which do not involve interactions with D522 (Fig. 5).

The residues lining the binding site described above are highly conserved among filoviruses, with the exception Marburg virus, suggesting that the antiviral activity these compounds against MARV will require additional research. As shown in Table 4, the anti-MARV activities of agents **3b** and **4b** were considerable higher than that observed against EBOV. Additional studies are required to localize the binding site on the MARV GP for the synthesized derivatives.

#### 4. Conclusion

In this study, we describe a series of (+)-camphor and (–)-borneol derivatives as potent filovirus enter inhibitors. The relationships between the structural properties of the synthesized ligands and their estimated affinities for EBOV GP using pseudotype viruses and *in silico* approach can be summarized as follows. (1) (–)-Borneol derivatives that contain a 4-N-substituted piperazine/piperidine heterocycle were the most potent against rVSV- $\Delta$ G-EboV-GP. (2) The longer aliphatic linker in both series (–)-borneol ester and (+)-camphor amide is associated with lower binding energies for EBOV GP and higher toxicity. (3) The configuration the 1,7,7-trimethylbicyclo[2.2.1]heptan moiety is important, and high activity and toxicity were discovered for (–)-borneol derivatives. The agents **3b** (**As-358**), **4b** and their hydrochloride salts **3b-HCl** and **4b-HCl** showed excellent antiviral activities using a “surrogate” system, which confirmed their inhibitory activity and in relation toward authentic filovirus. Based on the molecular docking and *in vitro* mutagenesis results, we suggest that the possible mechanism of action of the synthesized compounds is binding to the active site of EBOV glycoprotein, similar to that of the known inhibitor toremifene.

#### 5. Experimental section

##### 5.1. General

Reagents and solvents were purchased from commercial suppliers and used as received. Dry solvents were obtained according to standard procedures. GC MS was performed using a 7820A gas chromatograph (Agilent Technologies); a flame-ionization detector; a HP-5 capillary column (0.25 mm  $\times$  30 m 0.25  $\mu m$ ); and He as carrier gas (flow rate 2 mL/min, flow division 99:1). Optical rotation was assessed using a polAar 3005 spectrometer with a  $CHCl_3$  solution.  $^1H$  and  $^{13}C$  NMR spectra were recorded on Bruker spectrometers, including an AV-300 instrument at 300.13 MHz ( $^1H$ ) and 75.47 MHz ( $^{13}C$ ), an AV-400 instrument at 400.13 MHz ( $^1H$ ) and 100.61 MHz ( $^{13}C$ ), and a DRX-500 instrument at 500.13 MHz ( $^1H$ ) and 125.76 MHz ( $^{13}C$ ) in  $CDCl_3$ ; chemical shifts  $\delta$  were reported in ppm relative to residual  $CHCl_3$  [ $d(CHCl_3)$  7.24,  $d(CDCl_3)$  76.90 ppm], J in Hz. The structure of the products was determined by analyzing the  $^1H$  and  $^{13}C$  NMR spectra. HR-MS analyses were performed using

a DFS Thermo Scientific spectrometer in a full scan mode (0–500 *m/z*, 70 eV electron impact ionization, direct sample administration). Elemental analysis was performed using a Euro EA 3000 C,H,N,S-analyzer. Column chromatography was performed on silica gel (60–200  $\mu\text{m}$ , Macherey-Nagel). The purity of the target compounds was determined by gas chromatography. All of the target compounds reported in this study had a purity of  $\geq 95\%$ .

## 5.2. Chemistry

### 5.2.1. Syntheses of esters 3–7 *a-c*, 8 *a-b* and amides 18–20 *a-b*, 21c

Syntheses and structural characterization of the (–)-borneol ester **3–8 a-b** [14] and the ester **3-7c** as well as the (+)-camphor amides **18–20 a-b**, **21b** [20] were described in our previous publication.

### 5.2.2. Synthesis of (1*S*,2*R*,4*S*)-1,7,7-trimethylbicyclo[2.2.1]heptan-2-yl 5-chloropentanoate **2d**

To a solution of 5-chloropentanoic acid in dry  $\text{CH}_2\text{Cl}_2$ , excess oxalyl chloride and *N,N*-dimethylformamide (one drop) were added. Then, the mixture was stirred at room temperature for 3 h, after which the excess oxalyl chloride was removed using a rotary evaporator. The resulting 5-chloropentanoyl chloride was immediately used in a subsequent reaction.

5-Chloropentanoyl chloride (5 mmol) and  $\text{Et}_3\text{N}$  (5 mmol) was added to a solution of (–)-borneol (4.5 mmol) in  $\text{CH}_2\text{Cl}_2$  at 0–5 °C, after which the mixture was stirred at room temperature for 24 h. The reaction mixture was washed with brine and extracted with  $\text{CH}_2\text{Cl}_2$ . Then, the combined organic phase was dried over anhydrous  $\text{Na}_2\text{SO}_4$  and the solvent was removed. The crude product was then purified by flash CC (silica gel, eluent: hexane-ethyl acetate). Yield 58%; pale yellow oil.  $^1\text{H NMR}$  ( $\delta$ , ppm, J/Hz): 0.79 (3H, s, Me-9), 0.84 (3H, s, Me-10), 0.87 (3H, s, Me-8), 0.92 (1H, dd,  $^2J = 13.7$ ,  $J_{2\text{endo}, 1\text{exo}} = 3.4$ , H-2endo), 1.15–1.32 (2H, m, H-4endo, H-5exo), 1.60–1.94 (7H, m, H-3, H-4exo, H-5endo, H-13, H-14), 2.28–2.37 (3H, m, H-12, H-2exo), 3.49–3.58 (2H, m, H-15), and 4.83–4.88 (1H, m, H-1exo).

### 5.2.3. General synthetic procedure for compounds 3-4d

A mixture of chloride **2d** (2.5 mmol), piperidine/4-methylpiperidine (3 mmol),  $\text{Et}_3\text{N}$  (3 mmol) and 10 mL  $\text{CH}_2\text{Cl}_2$  were refluxed for 8 h. After completion, the mixture was washed with brine and extracted with  $\text{CH}_2\text{Cl}_2$ . The combined organic phase was dried over  $\text{Na}_2\text{SO}_4$ , and the solvent was removed in vacuo. The crude product was then purified by silica gel CC (eluent: hexane-ethyl acetate).

(1*S*,2*R*,4*S*)-1,7,7-trimethylbicyclo[2.2.1]heptan-2-yl 5-(piperidin-1-yl)pentanoate **3d**.

Yield 47%; pale yellow oil.  $^1\text{H NMR}$  ( $\delta$ , ppm, J/Hz): 0.79 (3H, s, Me-10), 0.84 (3H, s, Me-8), 0.87 (3H, s, Me-9), 0.91 (1H, dd,  $^2J = 12.9$ ,  $J_{2\text{endo}, 1\text{exo}} = 4.5$ , H-2endo), 1.14–1.31 (2H, m, H-4endo, H-5exo), 1.34–1.43 (2H, m, H-20), 1.45–1.76 (11H, m, H-3, H-4exo, H-5endo, H-13, H-14, H-18, H-19), 1.86–1.94 (1H, m, H-5endo), 2.23–2.41 (9H, m, H-2exo, H-12, H-15, H-16, H-17), 4.82–4.87 (1H, m, H-1exo).  $^{13}\text{C NMR}$  ( $\delta$ , ppm): 173.83 s (C-11), 79.50 d (C-1), 58.96 t (C-15), 54.49 t (C-16, C-17), 48.59 s (C-6), 47.64 s (C-7), 44.75 d (C-3), 36.70 t (C-2), 34.46 t (C-12), 27.91 t (C-4), 26.98 t (C-5), 26.31 t (C-14), 25.85 t (C-18, C-19), 24.34 t (C-20), 23.17 t (C-13), 19.57 q (Me-9), 18.70 q (Me-10), 13.38 q (Me-8). HR-MS: 321.2663 ( $\text{M}^+$ ,  $\text{C}_{20}\text{H}_{35}\text{O}_2\text{N}_1$ ; calcd 321.2662).

(1*S*,2*R*,4*S*)-1,7,7-trimethylbicyclo[2.2.1]heptan-2-yl 5-(4-methylpiperidin-1-yl)pentanoate **4d**.

Yield 51%; pale yellow oil.  $^1\text{H NMR}$  ( $\delta$ , ppm, J/Hz): 0.78 (3H, s, Me-10), 0.83 (3H, s, Me-8), 0.86 (3H, s, Me-9), 0.87 (3H, d,  $J = 6.6$  Hz, Me-21), 0.91 (1H, m, H-2endo), 1.12–1.31 (6H, m, H-4endo, H-5exo, H-18a, H-19a, H-14), 1.46–1.74 (8H, m, H-3, H-4exo, H-5endo, H-13,

H-18e, H-19e, H-20), 1.78–1.94 (3H, m, H-5endo, H-17a, H-16a), 2.23–2.35 (5H, m, H-2exo, H-12, H-15), 2.79–2.85 (2H, m, H-17e, H-16e), 4.81–4.86 (1H, m, H-1exo).  $^{13}\text{C NMR}$  ( $\delta$ , ppm): 173.47 s (C-11), 79.16 d (C-1), 58.27 t (C-15), 53.62 t (C-16, C-17), 48.26 s (C-6), 47.31 s (C-7), 44.42 d (C-3), 36.38 t (C-2), 34.13 t (C-12), 33.90 t (C-18, C-19), 30.39 d (C-20), 27.58 t (C-4), 26.66 t (C-5), 26.15 t (C-14), 22.84 t (C-13), 21.46 q (Me-21), 19.24 q (Me-9), 18.38 q (Me-10), 13.05 q (Me-8). HR-MS: 335.2817 ( $\text{M}^+$ ,  $\text{C}_{21}\text{H}_{37}\text{O}_2\text{N}_1$ ; calcd 335.2819).

### 5.2.4. Synthesis of the hydrochloride salts **3b-HCl** and **4b-HCl**

Excess hydrochloric acid was prepared by dissolving gaseous hydrogen chloride in  $\text{Et}_2\text{O}$ , which was added to solutions of compounds **3b** or **4b** in hexane. The resulting precipitate was collected by filtration, washed with hexane (10 mL), and then dried to yield **3b-HCl** and **4b-HCl**, respectively.

1-(3-Oxo-3-((1*S*,2*R*,4*S*)-1,7,7-trimethylbicyclo[2.2.1]heptan-2-yloxy)propyl)piperidinium chloride **3b-HCl**.

Yield 91%; white powder.  $^1\text{H NMR}$  ( $\delta$ , ppm, J/Hz): 0.75 (3H, c, Me-10), 0.81 (3H, c, Me-8), 0.83 (3H, c, Me-9), 0.89 (1H, dd,  $^2J = 13.7$ ,  $J_{2\text{endo}, 1\text{exo}} = 3.5$ , H-2endo), 1.12–1.29 (2H, m, H-4endo, H-5exo), 1.32–1.44 (1H, m, H-17a), 1.60–1.64 (1H, m, H-3), 1.64–1.74 (1H, m, H-4exo), 1.75–1.89 (4H, m, H-5endo, H-17e, H-15a, H-16a), 2.14–2.32 (3H, m, H-2exo, H-15e, H-17e), 2.57–2.69 (2H, m, H-11), 3.02–3.14 (2H, m, H-13a, H-14a), 3.17–3.26 (2H, m, H-13e, H-14e), 3.42–3.51 (2H, m, H-13), 4.79–4.85 (1H, m, H-1exo).  $^{13}\text{C NMR}$  ( $\delta$ , ppm): 170.37 s (C-11), 81.24 d (C-1), 53.35 and 53.29 t (C-14, C-15), 52.17 t (C-13), 48.56 s (C-6), 47.66 s (C-7), 44.54 d (C-3), 36.41 t (C-2), 28.92 t (C-4), 27.72 t (C-5), 26.76 t (C-12), 22.36 t (C-16, C-17), 21.79 t (C-18), 19.44 q (Me-9), 18.58 q (Me-10), 13.33 q (Me-8). Anal. Calcd for  $\text{C}_{18}\text{H}_{32}\text{ClNO}_2$ , C, 65.53; H, 9.78; Cl, 10.75; N, 4.25; O, 9.70. Found, %: C, 65.58; H, 9.68; Cl, 10.64; N, 4.30. M.p. = 245.1 °C.

4-Methyl-1-(3-oxo-3-((1*S*,2*R*,4*S*)-1,7,7-trimethylbicyclo[2.2.1]heptan-2-yloxy)propyl)piperidinium chloride **4b-HCl**.

Yield 85%; white powder.  $^1\text{H NMR}$  ( $\delta$ , ppm, J/Hz): 0.75 (3H, c, Me-10), 0.81 (3H, c, Me-8), 0.83 (3H, c, Me-9), 0.89 (1H, dd,  $^2J = 14.2$ ,  $J_{2\text{endo}, 1\text{exo}} = 3.4$ , H-2endo), 0.98 (3H, d,  $J = 5.7$  Hz, Me-19), 1.13–1.28 (2H, m, H-4endo, H-5exo), 1.49–2.01 (8H, m, H-3, H-4exo, H-5endo, H-16a, H-17a, H-16e, H-17e, H-18), 2.22–2.32 (1H, m, H-2exo), 2.57–2.69 (2H, m, H-11), 3.04–3.11 (2H, m, H-13a, H-14a), 3.17–3.25 (2H, m, H-13e, H-14e), 3.41–3.49 (2H, m, H-13), 4.80–4.85 (1H, m, H-1exo).  $^{13}\text{C NMR}$  ( $\delta$ , ppm): 170.38 s (C-11), 81.22 d (C-1), 53.23 and 53.17 t (C-14, C-15), 52.27 t (C-13), 48.55 s (C-6), 47.65 s (C-7), 44.52 d (C-3), 36.41 t (C-2), 30.58 t (C-16, C-17), 29.09 d (C-18), 28.95 t (C-4), 27.71 t (C-5), 26.75 t (C-11), 20.72 t (Me-19), 19.44 q (Me-9), 18.58 q (Me-10), 13.33 q (Me-8). Anal. Calcd for  $\text{C}_{19}\text{H}_{34}\text{ClNO}_2$ , C, 66.35; H, 9.96; Cl, 10.31; N, 4.07; O, 9.30. Found, %: C, 66.61; H, 11.09; Cl, 10.74; N, 4.09. M.p. = 231.9 °C.

### 5.2.5. General procedures A: syntheses of esters **8c**, **9-12a-c**

A1: A solution of (1*S*,2*R*,4*S*)-1,7,7-trimethylbicyclo[2.2.1]heptan-2-yl 2-chloroacetate (**2a**; 1 equiv),  $\text{Et}_3\text{N}$  (1 equiv) and the requisite secondary amine (1.5 equiv) in  $\text{CH}_2\text{Cl}_2$  was stirred at room temperature for 12 h. The resulting mixture was diluted with brine and extracted twice with  $\text{CH}_2\text{Cl}_2$ . Then, the combined organic layer was dried with anhydrous  $\text{Na}_2\text{SO}_4$  and evaporated. The crude residues were purified via silica gel column chromatography (hexane-ethyl acetate eluent).

A2: A solution of (1*S*,2*R*,4*S*)-1,7,7-trimethylbicyclo[2.2.1]heptan-2-yl 3-chloropropanoate (**2b**; 1 equiv),  $\text{Et}_3\text{N}$  (1 equiv) and the requisite secondary amine (1.5 equiv) in  $\text{CH}_2\text{Cl}_2$  was refluxed for 12–24 h. The resulting mixture was diluted with brine and extracted twice with  $\text{CH}_2\text{Cl}_2$ . Then, the combined organic layer was dried with anhydrous  $\text{Na}_2\text{SO}_4$  and evaporated. The crude residues were purified via silica gel column chromatography (hexane-ethyl

acetate eluent).

A3: A solution of (1S,2R,4S)-1,7,7-trimethylbicyclo[2.2.1]heptan-2-yl 4-chlorobutanoate (**2c**; 1 equiv), Et<sub>3</sub>N (1 equiv), DBU (one drop) and the requisite secondary amine (1.5 equiv) in CH<sub>3</sub>CN was refluxed for 18–24 h. The reaction mixture was concentrated under reduced pressure, diluted with brine and extracted twice with CH<sub>2</sub>Cl<sub>2</sub>. Then, the combined organic layer was dried with anhydrous Na<sub>2</sub>SO<sub>4</sub> and evaporated. The crude residues were purified via silica gel column chromatography (hexane-ethylacetate eluent).

*Ethyl 4-(4-oxo-4-((1S,2R,4S)-1,7,7-trimethylbicyclo[2.2.1]heptan-2-yloxy)butyl)piperazine-1-carboxylate 8c* (procedure A3). Yield 37%; pale yellow oil. <sup>1</sup>H NMR (δ, ppm, J/Hz): 0.79 (3H, s, Me-10), 0.83 (3H, s, Me-8), 0.87 (3H, s, Me-9), 0.91 (1H, dd, <sup>2</sup>J = 14.2, J<sub>2endo, 1exo</sub> = 3.2, H-2endo), 1.14–1.30 (5H, m, H-4endo, H-5exo, Me-21), 1.61–1.65 (1H, m, H-3), 1.65–1.74 (1H, m, H-4exo), 1.78 (2H, quint, J = 7.2, H-13), 1.84–1.92 (1H, m, H-5endo), 2.25–2.42 (9H, m, H-2exo, H-12, H-14, H-15, H-16), 3.39–3.47 (4H, br. s, H-17, H-18), 4.09 (2H, q, J = 7.05, H-20), 4.85 (1H, m, H-1exo). <sup>13</sup>C NMR (δ, ppm): 173.48 s (C-11), 155.31 s (C-19), 79.78 d (C-1), 61.26 t (C-20), 57.44 t (C-14), 52.64 t (C-15, C-16), 48.64 s (C-6), 47.68 s (C-7), 44.79 d (C-3), 43.25 t (C-17, C-18), 36.72 t (C-2), 32.19 t (C-12), 27.94 t (C-4), 27.02 t (C-5), 21.73 t (C-13), 19.57 q (Me-9), 18.70 q (Me-8), 14.53 q (Me-21), 13.41 q (Me-10). HR-MS: 380.2666 (M<sup>+</sup>, C<sub>21</sub>H<sub>36</sub>O<sub>4</sub>N<sub>2</sub>; calcd 380.2670).

*(1S,2S,4S)-1,7,7-Trimethylbicyclo[2.2.1]heptan-2-yl 2-(4-(2-hydroxyethyl)piperazin-1-yl)acetate 9a* (procedure A1). Yield 36%; pale yellow oil. <sup>1</sup>H NMR (δ, ppm, J/Hz): 0.76 (3H, s, Me-10), 0.80 (3H, s, Me-8), 0.83 (3H, s, Me-9), 0.91 (1H, dd, <sup>2</sup>J = 14.2, J<sub>2endo, 1exo</sub> = 3.2, H-2endo), 1.11–1.28 (2H, m, H-4endo, H-5exo), 1.59–1.73 (2H, m, H-4exo, H-3), 1.78–1.88 (1H, m, H-5endo), 2.23–2.35 (1H, m, H-2exo), 2.43–2.67 (10H, br. s, H-13, H-14, H-15, H-16, H-17), 2.94 (1H, br. s, OH), 3.17 (2H, s, H-12), 3.54 (2H, t, J = 5.4, H-18), 4.87 (1H, m, H-1exo). <sup>13</sup>C NMR (δ, ppm): 170.34 s (C-11), 79.96 d (C-1), 59.09 t (C-18), 59.05 t (C-12), 57.47 t (C-17), 52.62 and 52.45 t (C-13, C-14, C-15, C-16), 48.50 s (C-6), 47.54 s (C-7), 44.55 d (C-3), 36.52 t (C-2), 27.75 t (C-4), 26.84 t (C-5), 19.45 q (Me-9), 18.58 q (Me-8), 13.32 q (Me-10). HR-MS: 324.2413 (M<sup>+</sup>, C<sub>18</sub>H<sub>32</sub>O<sub>3</sub>N<sub>2</sub>; calcd 324.2407).

*(1S,2R,4S)-1,7,7-trimethylbicyclo[2.2.1]heptan-2-yl 3-(4-(2-hydroxyethyl)piperazin-1-yl)propanoate 9b* (procedure A2). Yield 45%; pale yellow oil. <sup>1</sup>H NMR (δ, ppm, J/Hz): 0.78 (3H, s, Me-10), 0.82 (3H, s, Me-8), 0.85 (3H, s, Me-9), 0.93 (1H, dd, <sup>2</sup>J = 14.2, J<sub>2endo, 1exo</sub> = 3.2, H-2endo), 1.12–1.29 (2H, m, H-4endo, H-5exo), 1.60–1.64 (1H, m, H-3), 1.65–1.75 (1H, m, H-4exo), 1.81–1.91 (1H, m, H-5endo), 2.24–2.34 (1H, m, H-2exo), 2.38–2.72 (14H, br. s, H-12, H-13, H-14, H-15, H-16, H-17, H-18), 3.28 (1H, br. s, OH), 3.57–3.63 (2H, m, H-19), 4.85 (1H, m, H-1exo). <sup>13</sup>C NMR (δ, ppm): 172.47 s (C-11), 79.71 d (C-1), 59.20 t (C-19), 57.35 t (C-18), 53.38 t (C-13), 52.63 and 52.30 t (C-14, C-15, C-16, C-17), 48.59 s (C-6), 47.59 s (C-7), 44.64 d (C-3), 36.47 t (C-2), 32.54 t (C-12), 27.85 t (C-4), 26.92 t (C-5), 19.49 q (Me-9), 18.63 q (Me-8), 13.32 q (Me-10). Anal. Calcd for C<sub>19</sub>H<sub>24</sub>O<sub>3</sub>N<sub>2</sub>, C, 67.42; H, 10.12; N, 8.28. Found, %: C, 67.04; H, 9.88; N, 8.21.

*(1S,2R,4S)-1,7,7-trimethylbicyclo[2.2.1]heptan-2-yl 4-(4-(2-hydroxyethyl)piperazin-1-yl)butanoate 9c* (procedure A3). Yield 27%; pale yellow oil. <sup>1</sup>H NMR (δ, ppm, J/Hz): 0.77 (3H, s, Me-10), 0.82 (3H, s, Me-8), 0.85 (3H, s, Me-9), 0.90 (1H, dd, <sup>2</sup>J = 14.2, J<sub>2endo, 1exo</sub> = 3.2, H-2endo), 1.10–1.30 (2H, m, H-4endo, H-5exo), 1.59–1.64 (1H, m, H-3), 1.66–1.93 (4H, m, H-4exo, H-13, H-5endo), 2.27–2.36 (5H, m, H-2exo, H-12, H-14), 2.36–2.55 (10H, br. s, H-15, H-16, H-17, H-18, H-19), 2.82 (1H, br. s, OH), 3.56 (2H, t, J = 5.4, H-20), 4.83 (1H, m, H-1exo). <sup>13</sup>C NMR (δ, ppm): 173.58 s (C-11), 79.57 d (C-1), 59.18 t (C-20), 57.59 t (C-14), 57.46 t (C-19), 52.96 and 52.71 t (C-15, C-16, C-17, C-18), 48.57 s (C-6), 47.60 s (C-7), 44.71 d (C-3), 36.66 t (C-2), 32.38 t (C-12), 27.88 t (C-4), 26.95 t (C-5), 22.10 t (C-13), 19.52 q (Me-9), 18.65 q (Me-8), 13.36 q (Me-10). HR-MS:

352.2716 (M<sup>+</sup>, C<sub>20</sub>H<sub>36</sub>O<sub>3</sub>N<sub>2</sub>; calcd 352.2721).

*(1S,2R,4S)-1,7,7-trimethylbicyclo[2.2.1]heptan-2-yl 2-(4-(2-aminoethyl)piperazin-1-yl)acetate 10a* (procedure A1). Yield 25%; brown oil. <sup>1</sup>H NMR (δ, ppm, J/Hz): 0.76 (3H, s, Me-10), 0.80 (3H, s, Me-8), 0.84 (3H, s, Me-9), 0.91 (1H, dd, <sup>2</sup>J = 14.2, J<sub>2endo, 1exo</sub> = 3.2, H-2endo), 1.11–1.29 (2H, m, H-4endo, H-5exo), 1.59–1.73 (2H, m, H-4exo, H-3), 1.80–1.88 (1H, m, H-5endo), 2.08 (2H, br. s, NH<sub>2</sub>), 2.25–2.34 (1H, m, H-2exo), 2.37 (2H, t, J = 6.0, H-17), 2.39–2.62 (8H, br. s, H-13, H-14, H-15, H-16), 2.72 (2H, t, J = 6.0, H-18), 3.17 (2H, s, H-12), 4.87 (1H, m, H-1exo). <sup>13</sup>C NMR (δ, ppm): 170.55 s (C-11), 80.07 d (C-1), 60.92 t (C-17), 59.36 t (C-12), 52.91 and 52.88 t (C-13, C-14, C-15, C-16), 48.65 s (C-6), 47.69 s (C-7), 44.72 d (C-3), 38.66 t (C-18), 36.66 t (C-2), 27.89 t (C-4), 26.98 t (C-5), 19.58 q (Me-9), 18.71 q (Me-8), 13.44 q (Me-10). HR-MS: 323.2554 (M<sup>+</sup>, C<sub>18</sub>H<sub>33</sub>O<sub>2</sub>N<sub>3</sub>; calcd 323.2567).

*(1S,2R,4S)-1,7,7-trimethylbicyclo[2.2.1]heptan-2-yl 4-(4-(2-aminoethyl)piperazin-1-yl)butanoate 10c* (procedure A3). Yield 35%; brown oil. <sup>1</sup>H NMR (δ, ppm, J/Hz): 0.78 (3H, s, Me-10), 0.83 (3H, s, Me-8), 0.86 (3H, s, Me-9), 0.91 (1H, dd, <sup>2</sup>J = 14.2, J<sub>2endo, 1exo</sub> = 3.2, H-2endo), 1.13–1.30 (2H, m, H-4endo, H-5exo), 1.61–1.66 (1H, m, H-3), 1.66–1.94 (4H, m, H-4exo, H-13, H-5endo), 1.96–2.04 (2H, br. s, NH<sub>2</sub>), 2.26–2.56 (15H, m, H-2exo, H-12, H-14, H-15, H-16, H-17, H-18, H-19), 4.84 (1H, m, H-1exo). <sup>13</sup>C NMR (δ, ppm): 173.67 s (C-11), 79.66 d (C-1), 57.48 t (C-14), 56.12 t (C-19), 52.88 and 52.62 t (C-15, C-16, C-17, C-18), 48.60 s (C-6), 47.65 s (C-7), 44.71 d (C-3), 36.69 t (C-2), 34.29 t (C-20), 32.39 t (C-12), 27.91 t (C-4), 26.97 t (C-5), 22.08 t (C-13), 19.56 q (Me-9), 18.69 q (Me-8), 13.42 q (Me-10). Anal. Calcd for C<sub>20</sub>H<sub>37</sub>O<sub>2</sub>N<sub>3</sub>, C, 68.33; H, 10.61; N, 11.95. Found, %: C, 68.63; H, 10.07; N, 11.53.

*(1S,2R,4S)-1,7,7-trimethylbicyclo[2.2.1]heptan-2-yl 2-(4-benzylpiperazin-1-yl)acetate 11a* (procedure A1). Yield 42%; yellow oil. <sup>1</sup>H NMR (δ, ppm, J/Hz): 0.80 (3H, s, Me-10), 0.84 (3H, s, Me-8), 0.87 (3H, s, Me-9), 0.95 (1H, dd, <sup>2</sup>J = 13.7, J<sub>2endo, 1exo</sub> = 3.3, H-2endo), 1.14–1.31 (2H, m, H-4endo, H-5exo), 1.63–1.66 (1H, m, H-3), 1.68–1.76 (1H, m, H-4exo), 1.83–1.92 (1H, m, H-5endo), 2.27–2.37 (1H, m, H-2exo), 2.46–2.64 (8H, br. s, H-13, H-14, H-15, H-16), 3.20 (2H, s, H-12), 3.50 (2H, s, H-17), 4.91 (1H, m, H-1exo), 7.19–7.24 (1H, m, H-21), 7.27–7.30 (4H, m, H-19, H-20, H-22, H-23). <sup>13</sup>C NMR (δ, ppm): 170.56 s (C-11), 138.00 s (C-18), 129.04 d (C-19, C-23), 128.06 d (C-20, C-22), 126.88 d (C-21), 80.02 d (C-1), 62.83 t (C-17), 59.36 t (C-12), 52.86 and 52.73 t (C-13, C-14, C-15, C-16), 48.63 s (C-6), 47.67 s (C-7), 44.69 d (C-3), 36.64 t (C-2), 27.87 t (C-4), 26.96 t (C-5), 19.57 q (Me-9), 18.71 q (Me-8), 13.43 q (Me-10). HR-MS: 370.2614 (M<sup>+</sup>, C<sub>23</sub>H<sub>34</sub>O<sub>2</sub>N<sub>2</sub>; calcd 370.2615).

*(1S,2R,4S)-1,7,7-trimethylbicyclo[2.2.1]heptan-2-yl 3-(4-benzylpiperazin-1-yl)propanoate 11b* (procedure A2). Yield 45%; pale yellow oil. <sup>1</sup>H NMR (δ, ppm, J/Hz): 0.80 (3H, s, Me-10), 0.84 (3H, s, Me-8), 0.88 (3H, s, Me-9), 0.95 (1H, dd, <sup>2</sup>J = 13.7, J<sub>2endo, 1exo</sub> = 3.3, H-2endo), 1.15–1.31 (2H, m, H-4endo, H-5exo), 1.62–1.67 (1H, m, H-3), 1.66–1.76 (1H, m, H-4exo), 1.85–1.94 (1H, m, H-5endo), 2.26–2.36 (1H, m, H-2exo), 2.37–2.54 (10H, br. s, H-12, H-14, H-15, H-16), 2.65–2.69 (2H, m, H-13), 3.48 (2H, s, H-18), 4.86 (1H, m, H-1exo), 7.19–7.23 (1H, m, H-22), 7.26–7.30 (4H, m, H-20, H-21, H-23, H-24). <sup>13</sup>C NMR (δ, ppm): 172.74 s (C-11), 137.96 s (C-19), 129.08 d (C-20, C-24), 128.07 d (C-21, C-23), 126.89 d (C-22), 79.70 d (C-1), 62.92 t (C-18), 53.60 t (C-13), 52.91 and 52.75 t (C-14, C-15, C-16, C-17), 48.66 s (C-6), 47.66 s (C-7), 44.73 d (C-3), 36.54 t (C-2), 32.69 t (C-12), 27.91 t (C-4), 26.99 t (C-5), 19.58 q (Me-9), 18.71 q (Me-8), 13.38 q (Me-10). HR-MS: 384.2767 (M<sup>+</sup>, C<sub>24</sub>H<sub>36</sub>O<sub>2</sub>N<sub>2</sub>; calcd 384.2771).

*(1S,2R,4S)-1,7,7-trimethylbicyclo[2.2.1]heptan-2-yl 4-(4-benzylpiperazin-1-yl)butanoate 11c* (procedure A3). Yield 31%; yellow oil. <sup>1</sup>H NMR (δ, ppm, J/Hz): 0.79 (3H, s, Me-10), 0.84 (3H, s, Me-8), 0.87 (3H, s, Me-9), 0.92 (1H, dd, <sup>2</sup>J = 13.7, J<sub>2endo, 1exo</sub> = 3.3, H-2endo), 1.15–1.30 (2H, m, H-4endo, H-5exo), 1.62–1.66 (1H, m, H-3),

1.66–1.75 (1H, m, H-4exo), 1.79 (2H, quint, J = 7.4, H-13), 1.85–1.94 (1H, m, H-5endo), 2.26–2.37 (5H, m, H-2exo, H-12, H-14), 2.38–2.56 (8H, br. s, H-15, H-16, H-17, H-18), 3.48 (2H, s, H-19), 4.85 (1H, m, H-1exo), 7.19–7.23 (1H, m, H-23), 7.25–7.29 (4H, m, H-21, H-22, H-24, H-25). <sup>13</sup>C NMR (δ, ppm): 173.67 s (C-11), 137.96 s (C-20), 129.10 d (C-20, C-24), 128.05 d (C-21, C-23), 126.88 d (C-22), 79.60 d (C-1), 62.95 t (C-18), 57.60 t (C-14), 53.02 and 52.92 t (C-15, C-16, C-17, C-18), 48.62 s (C-6), 47.65 s (C-7), 44.77 d (C-3), 36.70 t (C-2), 32.52 t (C-12), 27.92 t (C-4), 27.00 t (C-5), 22.20 t (C-13), 19.57 q (Me-9), 18.71 q (Me-8), 13.41 q (Me-10). HR-MS: 398.2930 (M<sup>+</sup>, C<sub>25</sub>H<sub>38</sub>O<sub>2</sub>N<sub>2</sub>; calcd 398.2928).

(1*S*,2*R*,4*S*)-1,7,7-trimethylbicyclo[2.2.1]heptan-2-yl 2-(azepan-1-yl)acetate **12a** (procedure A1). Yield 51%; yellow oil. <sup>1</sup>H NMR (δ, ppm, J/Hz): 0.80 (3H, s, Me-10), 0.85 (3H, s, Me-8), 0.87 (3H, s, Me-9), 0.95 (1H, dd, <sup>2</sup>J = 13.7, J<sub>2endo, 1exo</sub> = 3.3, H-2endo), 1.15–1.34 (2H, m, H-4endo, H-5exo), 1.54–1.77 (12H, m, H-4endo, H-5exo, H-3, H-4exo, H-14, H-15, H-16, H-17), 1.87–1.95 (1H, m, H-5endo), 2.29–2.39 (1H, m, H-2exo), 2.78 (4H, t, J = 5.2, H-13, H-18), 3.40 (2H, s, H-12), 4.90 (1H, m, H-1exo). <sup>13</sup>C NMR (δ, ppm): 171.69 s (C-11), 80.01 d (C-1), 59.79 t (C-12), 54.93 t (C-13, C-18), 48.60 s (C-6), 47.67 s (C-7), 44.72 d (C-3), 36.71 t (C-2), 28.44 t (C-14, C-17), 27.89 t (C-4), 27.07 t (C-5), 26.87 t (C-15, C-16), 19.58 q (Me-9), 18.70 q (Me-8), 13.43 q (Me-10). HR-MS: 293.2348 (M<sup>+</sup>, C<sub>18</sub>H<sub>31</sub>O<sub>2</sub>N<sub>1</sub>; calcd 293.2349).

(1*S*,2*R*,4*S*)-1,7,7-trimethylbicyclo[2.2.1]heptan-2-yl 3-(azepan-1-yl)propanoate **12b** (procedure A2). Yield 47%; pale yellow oil. <sup>1</sup>H NMR (δ, ppm, J/Hz): 0.80 (3H, s, Me-10), 0.84 (3H, s, Me-8), 0.87 (3H, s, Me-9), 0.95 (1H, dd, <sup>2</sup>J = 13.7, J<sub>2endo, 1exo</sub> = 3.3, H-2endo), 1.14–1.30 (2H, m, H-4endo, H-5exo), 1.51–1.76 (12H, m, H-4endo, H-5exo, H-3, H-4exo, H-15, H-16, H-17, H-18), 1.87–1.96 (1H, m, H-5endo), 2.26–2.37 (1H, m, H-2exo), 2.47 (2H, t, J = 7.2, H-12), 2.59–2.65 (4H, m, H-14, H-19), 2.83 (2H, t, J = 7.2, H-13), 4.85 (1H, m, H-1exo). <sup>13</sup>C NMR (δ, ppm): 172.68 s (C-11), 79.33 d (C-1), 54.71 t (C-14, C-19), 53.36 t (C-13), 48.30 s (C-6), 47.33 s (C-7), 44.43 d (C-3), 36.26 t (C-2), 32.84 t (C-12), 27.63 t (C-15, C-18), 27.57 t (C-4), 26.68 t (C-5), 26.48 t (C-16, C-17), 19.25 q (Me-9), 18.39 q (Me-8), 13.03 q (Me-10). HR-MS: 307.2507 (M<sup>+</sup>, C<sub>19</sub>H<sub>33</sub>O<sub>2</sub>N<sub>1</sub>; calcd 307.2506).

(1*S*,2*R*,4*S*)-1,7,7-trimethylbicyclo[2.2.1]heptan-2-yl 4-(azepan-1-yl)butanoate **12c** (procedure A3). Yield 45%; yellow oil. <sup>1</sup>H NMR (δ, ppm, J/Hz): 0.79 (3H, s, Me-10), 0.84 (3H, s, Me-8), 0.87 (3H, s, Me-9), 0.92 (1H, dd, <sup>2</sup>J = 13.7, J<sub>2endo, 1exo</sub> = 3.3, H-2endo), 1.15–1.30 (2H, m, H-4endo, H-5exo), 1.51–1.66 (11H, m, H-4endo, H-5exo, H-3, H-16, H-17, H-18, H-19), 1.66–1.81 (3H, m, H-4exo, H-13), 1.87–1.95 (1H, m, H-5endo), 2.26–2.37 (3H, m, H-2exo, H-12), 2.48 (2H, t, J = 7.4, H-14), 2.58–2.64 (4H, m, H-15, H-20), 4.85 (1H, m, H-1exo). <sup>13</sup>C NMR (δ, ppm): 173.22 s (C-11), 80.01 d (C-1), 56.71 t (C-14), 54.71 t (C-15, C-20), 48.61 s (C-6), 47.67 s (C-7), 44.73 d (C-3), 36.65 t (C-2), 31.69 t (C-12), 27.88 t (C-4), 26.95 t (C-5), 26.84 t (C-16, C-19), 25.69 t (C-17, C-18), 21.14 t (C-13), 19.54 q (Me-9), 18.67 q (Me-8), 13.39 q (Me-10). HR-MS: 321.2659 (M<sup>+</sup>, C<sub>20</sub>H<sub>35</sub>O<sub>2</sub>N<sub>1</sub>; calcd 321.2662).

#### 5.2.6. Preparation of derivatives 13a and 14a

(1*S*,2*R*,4*S*)-1,7,7-trimethylbicyclo[2.2.1]heptan-2-yl 2-(dimethylamino)acetate **13a**. A solution of (1*S*,2*R*,4*S*)-1,7,7-trimethylbicyclo[2.2.1]heptan-2-yl 2-chloroacetate **2a** (6.5 mmol) and CH<sub>3</sub>CN (10 mL) was treated with excess of dimethylamine (2.5 mL, 40% wt.) solution in ethanol and K<sub>2</sub>CO<sub>3</sub> (7 mmol) was added. The mixture left for the night at room temperature. The precipitate was filtered off and the solvent was removed at reduced pressure. The crude product was purified by column chromatography silica gel eluent hexane/EtOAc 100/0 → 0/100. Yield 71%; pale yellow oil. <sup>1</sup>H NMR (δ, ppm, J/Hz): 0.79 (3H, s, Me-10), 0.83 (3H, s, Me-8), 0.86 (3H, s, Me-9), 0.93 (1H, dd, <sup>2</sup>J = 13.7, J<sub>2endo, 1exo</sub> = 3.3, H-2endo), 1.15–1.30

(2H, m, H-4endo, H-5exo), 1.61–1.74 (2H, m, H-3, H-4exo), 1.84–1.91 (1H, m, H-5endo), 2.32 (6H, s, Me-13, Me-14), 2.29–2.33 (1H, m, H-2exo), 3.15 (2H, s, H-12), 4.91 (1H, m, H-1exo). <sup>13</sup>C NMR (δ, ppm): 170.86 s (C-11), 79.88 d (C-1), 60.28 t (C-12), 48.61 s (C-6), 47.65 s (C-7), 45.00 q (Me-13, Me-14), 44.68 d (C-3), 36.61 t (C-2), 27.85 t (C-4), 26.98 t (C-5), 19.55 q (Me-9), 18.68 q (Me-8), 13.37 q (Me-10). HR-MS: 239.1884 (M<sup>+</sup>, C<sub>14</sub>H<sub>25</sub>O<sub>2</sub>N<sub>1</sub>; calcd 239.1880).

(1*S*,2*R*,4*S*)-1,7,7-trimethylbicyclo[2.2.1]heptan-2-yl 2-(diethylamino)acetate **14a**. A solution of **2a** (4.3 mmol) and CH<sub>3</sub>CN (10 mL) was treated with excess of diethylamine (6 mmol) and K<sub>2</sub>CO<sub>3</sub> (7 mmol) was added. The mixture left for the night at room temperature. The precipitate was filtered off and the solvent was removed at reduced pressure. The crude product was purified by column chromatography silica gel eluent hexane/EtOAc 100/0 → 0/100. Yield 65%; pale yellow oil. <sup>1</sup>H NMR (δ, ppm, J/Hz): 0.78 (3H, s, Me-10), 0.82 (3H, s, Me-8), 0.85 (3H, s, Me-9), 0.92 (1H, dd, <sup>2</sup>J = 13.7, J<sub>2endo, 1exo</sub> = 3.3, H-2endo), 1.03 (6H, t, J = 7.2, Me-15, Me-16), 1.14–1.29 (2H, m, H-4endo, H-5exo), 1.61–1.75 (2H, m, H-3, H-4exo), 1.85–1.92 (1H, m, H-5endo), 2.27–2.35 (1H, m, H-2exo), 2.63 (4H, q, J = 7.2, H-13, H-14), 3.31 (2H, s, H-12), 4.88 (1H, m, H-1exo). <sup>13</sup>C NMR (δ, ppm): 171.72 s (C-11), 79.78 d (C-1), 53.85 t (C-12), 48.55 s (C-6), 47.61 s (C-7), 47.54 t (C-13, C-14), 44.68 d (C-3), 36.68 t (C-2), 27.86 t (C-4), 27.04 t (C-5), 19.54 q (Me-9), 18.67 q (Me-8), 13.37 q (Me-10), 12.35 q (Me-15, Me-16). HR-MS: 267.2196 (M<sup>+</sup>, C<sub>16</sub>H<sub>29</sub>O<sub>2</sub>N<sub>1</sub>; calcd 267.2193).

#### 5.2.7. General synthetic procedures for the preparation of 13 b,c and 14 b,c

A solution of **2b** or **2c** (2.8 mmol) and CH<sub>3</sub>CN (7 mL) was treated with an excess of dimethylamine (1.5 mL 40% wt.) solution in ethanol (for the synthesis compounds **13b,c**) or diethylamine (for the synthesis compounds **14b,c**), and K<sub>2</sub>CO<sub>3</sub> (7 mmol) was added. The mixture was refluxed for 12, after which the precipitate was filtered off and the solvent was removed at reduced pressure. Then, CH<sub>2</sub>Cl<sub>2</sub> was added to the resulting mixture, after which the solution was diluted with brine and extracted twice with CH<sub>2</sub>Cl<sub>2</sub>. The combined organic layer was dried with anhydrous Na<sub>2</sub>SO<sub>4</sub> and evaporated. The crude residues were purified via silica gel column chromatography (hexane-ethylacetate eluent).

(1*S*,2*R*,4*S*)-1,7,7-trimethylbicyclo[2.2.1]heptan-2-yl 3-(dimethylamino)propanoate **13b**. Yield 53%; pale yellow oil. <sup>1</sup>H NMR (δ, ppm, J/Hz): 0.78 (3H, s, Me-10), 0.82 (3H, s, Me-8), 0.86 (3H, s, Me-9), 0.93 (1H, dd, <sup>2</sup>J = 13.7, J<sub>2endo, 1exo</sub> = 3.3, H-2endo), 1.14–1.30 (2H, m, H-4endo, H-5exo), 1.61–1.75 (2H, m, H-3, H-4exo), 1.85–1.94 (1H, m, H-5endo), 2.21 (6H, s, Me-14, Me-15), 2.25–2.35 (1H, m, H-2exo), 2.42–2.61 (4H, AB, J = 7.1, H-12, H-13), 4.85 (1H, m, H-1exo). <sup>13</sup>C NMR (δ, ppm): 172.63 s (C-11), 79.75 d (C-1), 54.78 t (C-13), 48.65 s (C-6), 47.66 s (C-7), 45.05 q (Me-14, Me-15), 44.82 d (C-3), 36.61 t (C-2), 33.17 t (C-12), 27.90 t (C-4), 27.03 t (C-5), 19.56 q (Me-9), 18.69 q (Me-8), 13.29 q (Me-10). HR-MS: 253.2033 (M<sup>+</sup>, C<sub>15</sub>H<sub>27</sub>O<sub>2</sub>N; calcd 253.2036).

(1*S*,2*R*,4*S*)-1,7,7-trimethylbicyclo[2.2.1]heptan-2-yl 4-(dimethylamino)butanoate **13c**. Yield 47%; pale yellow oil. <sup>1</sup>H NMR (δ, ppm, J/Hz): 0.79 (3H, s, Me-10), 0.83 (3H, s, Me-8), 0.86 (3H, s, Me-9), 0.91 (1H, dd, <sup>2</sup>J = 13.7, J<sub>2endo, 1exo</sub> = 3.3, H-2endo), 1.14–1.30 (2H, m, H-4endo, H-5exo), 1.60–1.75 (2H, m, H-3, H-4exo), 1.77–1.93 (3H, m, H-5endo, H-13), 2.28 (6H, s, Me-15, Me-16), 2.29–2.40 (5H, m, H-2exo, H-12, H-14), 4.84 (1H, m, H-1exo). <sup>13</sup>C NMR (δ, ppm): 173.68 s (C-11), 79.59 d (C-1), 58.70 t (C-14), 48.55 s (C-6), 47.61 s (C-7), 45.20 q (Me-15, Me-16), 44.69 d (C-3), 36.63 t (C-2), 32.26 t (C-12), 27.87 t (C-4), 26.92 t (C-5), 22.82 t (C-13), 19.54 q (Me-9), 18.67 q (Me-8), 13.36 q (Me-10). HR-MS: 267.1197 (M<sup>+</sup>, C<sub>16</sub>H<sub>29</sub>NO<sub>2</sub>; calcd 267.1193).

(1*S*,2*R*,4*S*)-1,7,7-trimethylbicyclo[2.2.1]heptan-2-yl 3-(diethylamino)propanoate **14b**. Yield 58%; pale yellow oil. <sup>1</sup>H NMR (δ, ppm,

J/Hz): 0.79 (3H, s, Me-10), 0.83 (3H, s, Me-8), 0.86 (3H, s, Me-9), 0.93 (1H, dd,  $^2J = 13.7$ ,  $J_{2endo, 1exo} = 3.3$ , H-2endo), 0.99 (6H, t,  $J = 7.2$ , Me-16, Me-17), 1.15–1.29 (2H, m, H-4endo, H-5exo), 1.61–1.64 (1H, m, H-3), 1.65–1.73 (1H, m, H-4exo), 1.86–1.92 (1H, m, H-5endo), 2.21 (6H, s, M = 14, Me-15), 2.26–2.34 (1H, m, H-2exo), 2.39–2.44 (2H, m, H-12), 2.48 (4H, q,  $J = 7.2$ , H-14, H-15), 2.74–2.80 (2H, m, H-13), 4.84 (1H, m, H-1exo).  $^{13}C$  NMR ( $\delta$ , ppm): 173.08 s (C-11), 79.59 d (C-1), 48.57 s (C-6), 48.23 t (C-13), 47.61 s (C-7), 46.51 t (C-14, C-15), 44.71 d (C-3), 36.56 t (C-2), 32.35 t (C-12), 27.86 t (C-4), 26.96 t (C-5), 19.54 q (Me-9), 18.68 q (Me-8), 13.33 q (Me-10), 11.70 q (Me-16, Me-17). HR-MS: 281.2348 ( $M^+$ ,  $C_{17}H_{31}O_2N_1$ ; calcd 281.2349).

(1*S*,2*R*,4*S*)-1,7,7-trimethylbicyclo[2.2.1]heptan-2-yl 4-(diethylamino)butanoate **14c**. Yield 42%; pale yellow oil.  $^1H$  NMR ( $\delta$ , ppm, J/Hz): 0.79 (3H, s, Me-10), 0.83 (3H, s, Me-8), 0.86 (3H, s, Me-9), 0.91 (1H, dd,  $^2J = 13.7$ ,  $J_{2endo, 1exo} = 3.3$ , H-2endo), 1.01 (6H, t,  $J = 7.2$ , Me-17, Me-18), 1.13–1.32 (2H, m, H-4endo, H-5exo), 1.61–1.82 (6H, m, H-4endo, H-5exo, H-3, H-4exo, H-13), 1.83–1.95 (1H, m, H-5endo), 2.25–2.37 (3H, m, H-2exo, H-12), 2.41–2.58 (6H, m, H-14, H-15, H-16), 4.85 (1H, m, H-1exo).  $^{13}C$  NMR ( $\delta$ , ppm): 173.75 s (C-11), 79.64 d (C-1), 51.86 t (C-14), 48.61 s (C-6), 47.66 s (C-7), 46.79 t (C-15, C-16), 44.79 d (C-3), 36.69 t (C-2), 32.37 t (C-12), 27.92 t (C-4), 27.00 t (C-5), 22.21 t (C-13), 19.57 q (Me-9), 18.70 q (Me-8), 13.37 q (Me-10), 11.40 q (Me-17, Me-18). HR-MS: 295.2513 ( $M^+$ ,  $C_{18}H_{33}NO_2$ ; calcd 295.2506).

2-(4-Ethylpiperazin-1-yl)-*N*-((1*R*,2*R*,4*R*)-1,7,7-trimethylbicyclo[2.2.1]heptan-2-yl)acetamide **21a**. A solution of 2-chloro-*N*-((1*R*,2*R*,4*R*)-1,7,7-trimethylbicyclo[2.2.1]heptan-2-yl)acetamide (**17a**; 1 equiv),  $Et_3N$  (1 equiv) and the 1-ethylpiperazine (1.5 equiv) in  $CH_2Cl_2$  was refluxed for 12 h. After completion, the mixture was washed with brine and extracted twice with  $CHCl_3$ . Then, the combined organic phase was dried over  $Na_2SO_4$ , and the solvent was removed in vacuo. The crude product was purified by silica gel column chromatography (eluent: hexane/ethyl acetate). Yield: 35%, yellow oil.  $^1H$  NMR ( $\delta$ , ppm, J/Hz): 0.77 (3H, s, Me-10), 0.80 (3H, s, Me-9), 0.89 (3H, s, Me-8), 1.05 (3H, t,  $J = 7.2$ , Me-18), 1.07–1.15 (1H, m, H-4endo), 1.21–1.30 (1H, m, H-5endo), 1.47–1.56 (2H, m, H-5exo, H-2endo), 1.69–1.72 (2H, m, H-4exo, H-3), 1.81 (1H, dd,  $J = 9.0$ , 13.2, H-2exo), 2.37 (2H, q,  $J = 7.2$ , H-17), 2.42–2.63 (8H, br. s, H-13, H-14, H-15, H-16), 2.94 (2H, AB-d,  $J = 4.2$ , H-12), 3.83 (1H, dt,  $J = 4.3$ , 8.6, H-1exo), 7.36 (1H, N-H).  $^{13}C$  NMR ( $\delta$ , ppm): 168.9 s (C-11), 61.2 t (C-12), 55.7 d (C-1), 53.3 t (C-15, C-16), 52.9 t (C-13, C-14), 52.1 t (C-17), 48.3 s (C-6), 46.9 s (C-7), 44.8 d (C-3), 39.1 t (C-2), 35.6 t (C-5), 26.9 t (C-4), 20.0 q, 20.1 q (Me-8, Me-9), 11.9 q (Me-10), 11.8 q (Me-18). HR-MS: 307.2614 ( $M^+$ ,  $C_{18}H_{33}O_1N_3$ ; calcd 307.2618).

4-Chloro-*N*-((1*R*,2*R*,4*R*)-1,7,7-trimethylbicyclo[2.2.1]heptan-2-yl)butanamide **17c**. Excess oxalyl chloride and *N,N*-dimethylformamide (one drop) were added to a solution of 4-chlorobutanoic acid in dry  $CH_2Cl_2$ . The mixture was stirred at room temperature for 4 h in an Ar atmosphere, after which the excess oxalyl chloride was removed using a rotary evaporator. The resulting 4-chlorobutanoyl chloride was immediately used in a subsequent reaction.

4-Chlorobutanoyl chloride (10 mmol) in  $CH_2Cl_2$  (5 ml) and  $Et_3N$  (10 mmol) to a solution of (+)-isobornyl amine (8 mmol) in  $CH_2Cl_2$  was added at 0–5 °C, and the mixture was stirred at room temperature for 24 h in an atmosphere of Ar. The reaction mixture was washed with brine and extracted with  $CH_2Cl_2$ . Then, the combined organic phase was dried over anhydrous  $Na_2SO_4$  and the solvent was removed. The resulting amide was used in a subsequent reaction without purification. Yield 62%; yellow solid.  $^1H$  NMR ( $\delta$ , ppm, J/Hz): 0.78 (3H, s, Me-10), 0.79 (3H, s, Me-9), 0.86 (3H, s, Me-8), 1.06–1.14 (1H, m, H-4endo), 1.18–1.27 (1H, m, H-5endo), 1.47–1.56 (2H, m, H-5exo, H-2endo), 1.60–1.71 (2H, m, H-4exo, H-3), 1.80 (1H, dd,  $J = 9.0$ , 13.2, H-2exo), 2.02–2.07 (2H, m, H-13), 2.28–2.33 (2H, m, H-12), 3.51–3.61 (2H, m, H-14), (3.86 (1H, dt,

$J = 4.3$ , 8.6, H-1exo), 5.55 (1H, N-H).

#### 5.2.8. General procedure for syntheses of amides 18–21c

A solution comprising **17c** (1.5 mmol) in acetonitrile (15 ml), the corresponding amine (2 mmol),  $Et_3N$  (2 mmol) and one drop of DBU were refluxed for 12 h. After completion, the mixture was concentrated in a vacuum. Brine and  $CHCl_3$  were added to the residue, and then the mixture was extracted twice with  $CHCl_3$ . Then, the combined organic phase was dried over  $Na_2SO_4$ , and the solvent was removed in vacuo. The crude product was purified by silica gel CC (eluent: hexane-ethyl acetate).

4-Morpholino-*N*-((1*R*,2*R*,4*R*)-1,7,7-trimethylbicyclo[2.2.1]heptan-2-yl)butanamide **18c**. Yield: 46%, yellow oil.  $^1H$  NMR ( $\delta$ , ppm, J/Hz): 0.79 (6H, s, Me-10, Me-9), 0.86 (3H, s, Me-8), 1.07–1.15 (1H, m, H-4endo), 1.19–1.28 (1H, m, H-5endo), 1.44–1.56 (2H, m, H-5exo, H-2endo), 1.60–1.71 (2H, m, H-4exo, H-3), 1.75–1.85 (3H, m, H-2exo, H-13), 2.16 (2H, t,  $J = 7.3$ , H-12), 2.32 (2H, t,  $J = 7.2$ , H-14), 2.35–2.41 (2H, br. s, H-15, H-16), 3.64–3.68 (4H, m, H-17, H-18), 3.87 (1H, dt,  $J = 4.9$ , 9.2, H-1exo), 5.44 (1H, N-H).  $^{13}C$  NMR ( $\delta$ , ppm): 171.6 s (C-11), 66.8 t (C-17, C-18), 57.5 t (C-14), 56.4 d (C-1), 53.5 t (C-15, C-16), 48.3 s (C-6), 46.9 s (C-7), 44.8 d (C-3), 39.0 t (C-2), 35.8 t (C-5), 34.3 t (C-12), 26.8 t (C-4), 22.3 t (C-13), 20.2 q, 20.1 q (Me-8, Me-9), 11.6 q (Me-10). HRMS: calcd for  $C_{18}H_{32}O_2N_2$ : 308.2458; found: 308.2451.

4-(4-Methylpiperazin-1-yl)-*N*-((1*R*,2*R*,4*R*)-1,7,7-trimethylbicyclo[2.2.1]heptan-2-yl)butanamide **19c**. Yield: 28%, brown oil.  $^1H$  NMR ( $\delta$ , ppm, J/Hz): 0.78 (6H, s, Me-10, Me-9), 0.85 (3H, s, Me-8), 1.07–1.14 (1H, m, H-4endo), 1.20–1.28 (1H, m, H-5endo), 1.45–1.55 (2H, m, H-5exo, H-2endo), 1.60–1.70 (2H, m, H-4exo, H-3), 1.74–1.84 (3H, m, H-2exo, H-13), 2.15 (2H, t,  $J = 6.8$ , H-12), 2.26 (3H, s, H-19), 2.10–2.53 (10H, m, H-14, H-15, H-16, H-17, H-18), 3.85 (1H, dt,  $J = 4.3$ , 8.6, H-1exo), 5.56 (1H, N-H).  $^{13}C$  NMR ( $\delta$ , ppm): 171.7 s (C-11), 57.0 t (C-14), 56.4 d (C-1), 54.8 t (C-15, C-16), 52.7 t (C-17, C-18), 48.3 s (C-6), 46.9 s (C-7), 45.8 q (Me-19), 44.7 d (C-3), 38.9 t (C-2), 35.7 t (C-5), 34.3 t (C-12), 26.8 t (C-4), 22.5 t (C-13), 20.2 q, 20.1 q (Me-8, Me-9), 11.6 q (Me-10). HR-MS: 321.2775 ( $M^+$ ,  $C_{19}H_{35}O_1N_3$ ; calcd 321.2775).

4-(4-Methylpiperidin-1-yl)-*N*-((1*R*,2*R*,4*R*)-1,7,7-trimethylbicyclo[2.2.1]heptan-2-yl)butanamide **20c**. Yield: 36%, yellow oil.  $^1H$  NMR ( $\delta$ , ppm, J/Hz): 0.79 (6H, s, Me-10, Me-9), 0.86 (3H, s, Me-8), 0.88 (3H, d,  $J = 6.5$ , Me-20), 1.08–1.30 (5H, m, H-4endo, H-5endo, H-18a, H-19, H-19a), 1.45–1.72 (6H, m, H-5exo, H-2endo, H-4exo, H-3, H-17e, H-18e), 1.75–1.92 (5H, m, H-2exo, H-15a, H-16a, H-13), 2.15 (2H, t,  $J = 6.8$ , H-12), 2.28–2.36 (2H, m, H-14), 2.78–2.88 (2H, m, H-14e, H-15e), 3.87 (1H, dt,  $J = 4.9$ , 9.2, H-1exo), 5.57 (1H, N-H).  $^{13}C$  NMR ( $\delta$ , ppm): 171.9 s (C-11), 57.5 t (C-14), 56.4 d (C-1), 53.9 t (C-15, C-16), 48.4 s (C-6), 46.9 s (C-7), 44.8 d (C-3), 39.0 t (C-2), 35.9 t (C-5), 34.6 t (C-18, C-17), 34.1 (C-12), 30.7 d (C-19), 26.9 t (C-4), 22.9 t (C-13), 21.7 q (Me-20), 20.2 q, 20.1 q (Me-8, Me-9), 11.6 q (Me-10). HR-MS: 320.2819 ( $M^+$ ,  $C_{20}H_{36}O_1N_2$ ; calcd 320.2822).

4-(4-Ethylpiperazin-1-yl)-*N*-((1*R*,2*R*,4*R*)-1,7,7-trimethylbicyclo[2.2.1]heptan-2-yl)butanamide **21c**. Yield: 32%, yellow oil.  $^1H$  NMR ( $\delta$ , ppm, J/Hz): 0.79 (6H, s, Me-10, Me-9), 0.86 (3H, s, Me-8), 1.05 (3H, t,  $J = 7.1$ , Me-20), 1.08–1.15 (1H, m, H-4endo), 1.21–1.29 (1H, m, H-5endo), 1.45–1.56 (2H, m, H-5exo, H-2endo), 1.61–1.71 (2H, m, H-4exo, H-3), 1.74–1.86 (3H, m, H-2exo, H-13), 2.15 (2H, t,  $J = 6.8$ , H-12), 2.28–2.58 (12H, m, H-14, H-15, H-16, H-17, H-18, H-19), 3.87 (1H, dt,  $J = 4.3$ , 8.6, H-1exo), 5.48 (1H, N-H).  $^{13}C$  NMR ( $\delta$ , ppm): 171.8 s (C-11), 56.9 t (C-14), 56.4 d (C-1), 52.8 t (C-15, C-16), 52.6 t (C-17, C-18), 52.2 t (C-19), 48.3 s (C-6), 46.9 s (C-7), 44.7 d (C-3), 39.0 t (C-2), 35.7 t (C-5), 34.5 t (C-12), 26.8 t (C-4), 22.7 t (C-13), 20.2 q, 20.1 q (Me-8, Me-9), 11.8 q (Me-20), 11.6 q (Me-10). HR-MS: 335.2934 ( $M^+$ ,  $C_{20}H_{37}O_1N_3$ ; calcd 335.2931).

#### 5.2.9. Synthesis of (+)- and (–)-isoborneols

(+)-Camphor (3.00 g, 20 mmol) or (–)-camphor (3.00 g,

20 mmol) was dissolved in methanol (20 mL), and sodium borohydride (3.5 g, 92 mmol) was added in portions. The solution was cooled to  $-30^{\circ}\text{C}$  and stirred for 3 h and then for 4 h at room temperature. The reaction mixture was then diluted with 2 M HCl and extracted with diethyl ether. Subsequently, the combined organic extracts were washed with brine (20 mL), dried with anhydrous  $\text{Na}_2\text{SO}_4$  and evaporated to yield the white solid products (+)-isborneol (14 mmol, 71%) and (–)-isborneol (15 mmol, 75%), the  $^1\text{H}$  NMR spectrum for which showed it to consisted of two diastereomers in an approximately 9:1 ratio. The diastereomers were separated by silica gel column chromatography (eluent: hexane/ethyl acetate). NMR spectra for (+)-isborneol and (–)-isborneol agreed with those presented in the literature [24]. (+)-Isborneol  $[\alpha]_D^{26} = -20$  (c 0.5,  $\text{CHCl}_3$ ), mp = 203.0–204.9. (–)-Isborneol  $[\alpha]_D^{26} = 23.3$  (c 0.3,  $\text{CHCl}_3$ ), mp = 197.8.

#### 5.2.10. Synthesis of (1R,2R,4R)- and (1S,2S,4S)-1,7,7-trimethylbicyclo[2.2.1]heptan-2-yl 2-chloroacetates [(1R,2R,4R)-22 and (1S,2S,4S)-22]

Chloroacetyl chloride (2.4 mL, 0.03 mol) was added to a mixture of (+)-isborneol or (–)-isborneol (3.00 g, 0.02 mol) and  $\text{Et}_3\text{N}$  (2.8 mL, 0.02 mol) in 20 mL dry  $\text{CH}_2\text{Cl}_2$  at  $15\text{--}18^{\circ}\text{C}$ , after which the mixture was stirred at room temperature (with slight heating for (–)-isborneol) for 12 h. The reaction mixture was washed with brine and extracted with  $\text{CH}_2\text{Cl}_2$ . Then, the combined organic phase was dried over anhydrous  $\text{Na}_2\text{SO}_4$  and the solvent was removed. The resulting product was used in a further reaction without purification.

**(1R,2R,4R)-22.** Yield: 55%, pale yellow oil.  $^1\text{H}$  NMR ( $\delta$ , ppm, J/Hz): 0.82 (3H, s), 0.83 (3H, s), 0.85–0.88 (1H, m), 0.95 (3H, s), 1.00–1.17 (2H, m), 1.49–1.59 (1H, m), 1.60–1.70 (1H, m), 1.71–1.81 (2H, m), 4.00 (2H, s), 4.70–4.75 (1H, m). HR-MS: 230.1066 ( $\text{M}^+$ ,  $\text{C}_{12}\text{H}_{19}\text{O}_2\text{Cl}$ ; calcd 230.1068).  $[\alpha]_D^{25} = -68.5$  (c 0.9,  $\text{CHCl}_3$ ).

**(1S,2S,4S)-22.** Yield: 43%, colorless oil.  $^1\text{H}$  NMR ( $\delta$ , ppm, J/Hz): 0.82 (3H, s), 0.84 (3H, s), 0.85–0.88 (1H, m), 0.95 (3H, s), 1.00–1.16 (2H, m), 1.50–1.59 (1H, m), 1.63–1.70 (1H, m), 1.71–1.81 (2H, m), 4.00 (2H, s), 4.70–4.74 (1H, m). HR-MS: 230.1066 ( $\text{M}^+$ ,  $\text{C}_{12}\text{H}_{19}\text{O}_2\text{Cl}$ ; calcd 230.1068).

#### 5.2.11. General procedure for the nucleophilic substitution (1R,2R,4R)-22 and (1S,2S,4S)-22 with piperidin and 4-methylpiperidin

The requisite amine (1.1 mmol) piperidin or 4-methylpiperidin was added to a solution of **(1R,2R,4R)-22** or **(1S,2S,4S)-22** (0.2 g, 0.9 mmol) and  $\text{Et}_3\text{N}$  (0.1 mL, 0.9 mmol) in  $\text{CH}_2\text{Cl}_2$  (5 mL), and the mixture was stirred at room temperature for 12 h. The reaction mixture was washed with brine and extracted with  $\text{CH}_2\text{Cl}_2$ . Then, the combined organic phase was dried over anhydrous  $\text{Na}_2\text{SO}_4$  and the solvent was removed. The crude products were purified by column chromatography on silica gel using a gradient of EtOAc (1–15%) in hexane.

**(1R,2R,4R)-1,7,7-trimethylbicyclo[2.2.1]heptan-2-yl 2-(piperidin-1-yl)acetate (1R,2R,4R)-23.**  $^1\text{H}$  NMR ( $\delta$ , ppm, J/Hz): 0.79 and 0.80 (6H, s, Me-8, Me-9), 0.93 (3H, s, Me-8), 1.99–1.15 (2H, m, H-4endo, H-5endo), 1.34–1.81 (11H, m, H-15, H-16, H-17, H-3, H-4exo, H-5exo, H-2endo, H-2exo), 2.43–2.51 (4H, m, H-13, H-14), 3.11 (2H, s, H-12), 4.68 (1H, m, H-1exo).  $^{13}\text{C}$  NMR ( $\delta$ , ppm): 169.82 s (C-11), 80.54 d (C-1), 59.94 t (S-12), 53.73 t (C-13, C-14), 48.22 s (C-6), 47.46 s (C-7), 44.55 d (C-3), 38.33 t (C-2), 33.21 t (C-5), 26.54 t (C-4), 25.39 t (C-15, C-17), 23.47 t (C-16), 19.64 q and 19.46 q (Me-8 and Me-9), 11.08 q (Me-10).  $[\alpha]_D^{22} = -46.1$  (c 0.4,  $\text{CHCl}_3$ ). HR-MS: 279.2191 ( $\text{M}^+$ ,  $\text{C}_{17}\text{H}_{29}\text{O}_2\text{N}$ ; calcd 279.2193).

**(1R,2R,4R)-1,7,7-trimethylbicyclo[2.2.1]heptan-2-yl 2-(4-methylpiperidin-1-yl)acetate (1R,2R,4R)-24.** Yield: 48%, pale

yellow oil.  $^1\text{H}$  NMR ( $\delta$ , ppm, J/Hz): 0.80 (6H, s, Me-8, Me-9), 0.88 (3H, d, J = 5.8, Me-18), 0.94 (3H, s, Me-8), 1.00–1.16 (2H, m, H-4endo, H-5endo), 1.21–1.34 (3H, m, H-15a, H-17, H-16a), 1.46–1.82 (7H, m, H-15e, H-16e, H-3, H-4exo, H-5exo, H-2endo, H-2exo), 2.07–2.16 (2H, m, H-13a, H-14a), 2.30 (1H, m, H-2exo), 2.82–2.91 (2H, m, H-13e, H-14e), 3.13 (2H, s, H-12), 4.69 (1H, m, H-1exo).  $^{13}\text{C}$  NMR ( $\delta$ , ppm): 170.19 s (C-11), 80.87 d (C-1), 59.91 t (C-12), 53.54 and 53.50 t (C-13, C-14), 48.55 s (C-6), 46.79 s (C-7), 44.86 d (C-3), 38.65 t (C-2), 34.05 t (C-15, C-16), 33.54 t (C-5), 30.20 d (C-17), 26.87 t (C-4), 21.76 q (Me-18), 19.97 q and 19.79 q (Me-8, Me-9), 11.42 q (Me-10).  $[\alpha]_D^{25} = -38.8$  (c 0.5,  $\text{CHCl}_3$ ). HR-MS: 293.2345 ( $\text{M}^+$ ,  $\text{C}_{18}\text{H}_{31}\text{NO}_2$ ; calcd 293.2349).

**(1S,2S,4S)-1,7,7-trimethylbicyclo[2.2.1]heptan-2-yl 2-(piperidin-1-yl)acetate (1S,2S,4S)-23.**  $^1\text{H}$  and  $^{13}\text{C}$  NMR specters and HRMS coincide with compound **(1R,2R,4R)-23**.  $[\alpha]_D^{22} = 31$  (c 0.4,  $\text{CHCl}_3$ ).

**(1S,2S,4S)-1,7,7-trimethylbicyclo[2.2.1]heptan-2-yl 2-(4-methylpiperidin-1-yl)acetate (1S,2S,4S)-24.**  $^1\text{H}$  and  $^{13}\text{C}$  NMR specters and HRMS coincide with compound **(1R,2R,4R)-24**.  $[\alpha]_D^{22} = 38$  (c 0.4,  $\text{CHCl}_3$ ).

### 5.3. Molecular modeling

Molecular modeling was carried out in the Schrodinger Maestro visualization environment using applications from the Schrodinger Small Molecule Drug Discovery Suite 2016-1 package. Three-dimensional structures of the derivatives were empirically obtained in the LigPrep application using the OPLS3 force field [25]. For calculations, the XRD models (PDB IDs 6F5U, 6F6N, and 6F6I) of EBOV GP inhibited by various drugs from the Protein Data Bank were chosen [12]. To model a possible mechanism of inhibition for the selected target, molecular docking of new compounds was performed at the binding site of EBOV GP using Glide [26]. The search area for docking was selected according to the size of known inhibitors. Docking was performed in comparison with known inhibitors. The three-dimensional structures of inhibitors were obtained in the PubChem database and prepared in the LigPrep application. Noncovalent interactions of molecules in the binding site were visualized using Biovia Discovery Studio Visualizer and Schrodinger Maestro.

### 5.4. Biological assays

#### 5.4.1. Cell lines

HEK293FT and HEK293T cells were maintained in DMEM (Invitrogen) containing 10% fetal bovine serum (FBS; Gibco), 0.6 mg/mL L-glutamine (Invitrogen) and 50  $\mu\text{g}/\text{mL}$  gentamicin.

#### 5.4.2. Production of rVSV- $\Delta\text{G}$ pseudotyped EboV-GP (Y517A-EboV-GP, D522A-EboV-GP, and M548A-EboV-GP)

To generate Ebola glycoprotein (or variants with amino acid substitutions) pseudotyped VSVs containing the firefly luciferase gene, 293FT cells grown in a T75 were transfected with a pGPE plasmid (pGPE-Y517A, pGPE-D522A, or pGPE-M548A) using the  $\text{CaCl}_2$  method (23  $\mu\text{g}$  of plasmid per cell monolayer in a T75 culture vial). After 16 h the culture medium was replaced, and a suspension of VSV of the firefly luciferase gene pseudotyped by surface VSV glycoprotein G (rVSV- $\Delta\text{G}$ -G) was added to the cells [27]. After 6 h, the cells were washed, and the medium was exchanged with fresh medium. Pseudoviruses were harvested after 48 h by filtering the culture medium through a 0.45- $\mu\text{m}$  filter after centrifugation to remove cell debris. Pseudoviruses were stored at  $-80^{\circ}\text{C}$ , and their functional activity was determined using a HEK293T cell culture, with the luminescence level recorded using a Stat Fax 4400 luminometer.

### 5.4.3. Plasmids

The plasmid pGPE containing the Ebola virus surface glycoprotein gene of the Mayinga strain was obtained by inserting the synthesized gene into the vector pcDNA3.1. Prior to synthesis, codon optimization of the GP gene was performed.

To construct the plasmids pGPE-Y517A, pGPE-D522A and pGPE-M548A, site-directed mutagenesis was performed. To this end, the primers Ebo-F and Ebo-R were designed that flank the GPE gene sequence. Then, for each of the amino acid substitutions, the corresponding pairs of primers containing nucleotide substitutions introducing the desired amino acid change (517-F, 517-R, 522-F, 522-R, 548-F and 548-R) were designed. PCR was performed with primer pairs Ebo-F, 517-R (522-R, 548-R) and Ebo-R, 517-F (522-F, 548-F). PCR products were purified, and amplified annealing was performed using the primers Ebo-F and Ebo-R. The resulting product was inserted into the original plasmid pGPE.

Oligonucleotide name	Nucleotide sequence
Ebo-F	5'-ttttctagcggccaccatggcgcttacagaaatattgcagtt-3'
Ebo-R	5'-tttttctggcggaaactaaaagacaaattgcatatac-3'
517-R	5'-cctgagtagtcaggcatgaaattagggttcattgg-3'
517-F	5'-ccaatgcaaccctaatttacatgctggactactcagg-3'
522-F	5'-atttaccattactggactactcagcttgaaggtgctgcaatcg-3'
522-R	5'-ccgattgcagcacttcaagctgagtagtccagtaagttaaat-3'
548-F	5'-gggaattacatagagggctcgcgcacaatcaagatgttta-3'
548-R	5'-taaacattcttgattgtgcgagccctctatgtaaaatccc-3'

### 5.4.4. Pseudotype virus entry inhibition assay

Viral entry inhibition assays were performed using HEK293T cells. Cells were seeded in 96-well plates (100 µl at a density of 10<sup>5</sup> cells per ml) one day before analysis. The following day, potential inhibitor compounds were titrated in 96-well round-bottom plates at a dilution of 1:4. Next, 10-µl aliquots of pseudoviruses (10<sup>5</sup> PFU) were added to each well, and the mixtures were incubated for 1 h in a CO<sub>2</sub> incubator at 37 °C under an atmosphere with 5% CO<sub>2</sub>. After incubation, an aliquot of each mixture was added to a monolayer of cells. As a negative control, cells were treated with the same volume of medium as that used for the pseudovirus compound mixture was added to cells. After incubating in a CO<sub>2</sub> incubator for 48 h, the luminescence level was measured using a Stat Fax 4400 plate luminometer. To this end, the medium was carefully removed from the wells, the cells were washed with 100 µl/well of PBS and then 25 µl of Luciferase Cell Culture Lysis Buffer (Promega) was added. After 5 min, 50 µl of Luciferase Assay Reagent (Promega) was added. The percentage of inhibition was evaluated by determining the degree of decrease in luminescence in the wells with the compounds relative to the control wells (cells with the virus without compounds). All test compounds were dissolved in dimethylsulfoxide (DMSO) at a concentration of 10 mg/ml and used at a final concentration of 375 to 0.02 µg/ml.

### 5.4.5. Cytotoxicity assays

MTT reduction was used to study cytotoxicity of the compounds.[28] Briefly, series of two-fold dilutions of each compound (15.6–1000 µM) in 10% DMEM were prepared in 96-well plates. HEK293T cells (100 µl at a density of 10<sup>5</sup> cells per ml) were added and incubated for 48 h at 37 °C in 5% CO<sub>2</sub>. Then 20 µl (1/10 vol) of a solution of 3-(4,5-dimethylthiazolyl-2)-2,5-diphenyltetrazolium bromide (Sigma) (5 mg/ml) in phosphate-buffered saline was added to each well. After 2 h incubation, the solution was removed from wells and DMSO (100 µl per well) was added to dissolve the formazan crystals. The optical density of cells was then measured

on a Model 680 Microplate (Bio-Rad) Reader at 535 nm and plotted against concentration of the compounds. Each concentration was tested in three parallels. The 50% cytotoxic dose (CC<sub>50</sub>) of each compound (i.e., the compound concentration that causes the death of 50% cells in a culture, or decreasing the optical density twice as compared to the control wells) was calculated from the data obtained.

### 5.4.6. Ebola and Marburg Virus Infections under BSL-4 conditions

EBOV (strain Zaire) and MARV (strain Popp) were obtained from the State Collection of Viral Infections and Rickettsioses Agents of SRC VB Vector suspended in culture supernatant. Titer EBOV was 4.5 ± 0.75 lgTCD<sub>50</sub>/ml, titer MARV was 5.3 ± 0.63 lgTCD<sub>50</sub>/ml. Anti-EBOV and anti-MARV assays were conducted at SRC VB Vector in a maximum containment facility (BSL-4). Vero cell culture (African green monkey kidney cell line) were seeded into 96-well plates and were grown into confluent monolayers. Series of 3-fold dilutions of each compound (previously dissolved in 100% DMSO) in DMEM medium were prepared starting of 300 µg/ml. Six decreasing concentrations were prepared of each inhibitors. The compounds were added of 100 µL/well. Viruses were used at a multiplicity of infection of 0.01 (equivalent to a dose of 100 TCID<sub>50</sub> per well). For the treatment assay, 100 µL of diluted virus (100 TCID<sub>50</sub>) was added. For cytotoxicity assay to each well was added 100 µL DMEM medium. After incubation at 37 °C and 5% CO<sub>2</sub> for 10 days, neutral red was then added. The absorbance was measured at 490 nm using a microplate reader (Thermo Scientific Multiskan FC). The 50% cytotoxicity concentration (CC<sub>50</sub>) and 50% inhibitory concentration (IC<sub>50</sub>) was calculated using SOFTmax PRO 4.0 with the 4-parameter analysis method. Each inhibitor was analyzed at least 3 times.

### 5.4.7. Acute toxicity

ICR mice weighing 22–25 g were obtained from the animal facility of SRC VB Vector, Rospotrebnadzor and maintained under standard conditions with free access to food and water. All experiments were performed in accordance with the “European Convention for the Protection of Vertebrate Animals Used for Experimental and other Scientific Purposes”, 2010, and were approved by the Ethic Committee of the N.N. Vorozhtsov Institute of Organic Chemistry SB RAS (protocol No. 10/2019). The mice were weighed and randomly divided into groups (2 mice/group). Test compounds were administered by gavage (0.1 mL/10 g) at various doses, whereas the control groups received only solvent. Because of the lower water solubility of the compounds, a solution of DMSO in water (10%) was used as the solvent.

### Funding sources

This work was supported by a grant from the Russian Science Foundation 19-73-00125.

### Declaration of competing interest

The authors declare that they have no known competing financial interests or personal relationships that could have appeared to influence the work reported in this paper.

### Acknowledgment

The authors would like to acknowledge the Multi-Access Chemical Research Center SB RAS for spectral and analytical measurements.

## Appendix A. Supplementary data

Supplementary data to this article can be found online at <https://doi.org/10.1016/j.ejmech.2020.112726>.

## References

- [1] T. Goldstein, S.J. Anthony, A. Gbakima, B.H. Bird, J. Bangura, A. Tremeau-Bravard, M.N. Belaganahalli, H.L. Wells, J.K. Dhanota, E. Liang, M. Grodus, R.-K. Jangra, V.A. DeJesus, G. Lasso, B.R. Smith, A. Jambai, B.O. Kamara, S. Kamara, W. Bangura, C. Monagin, S. Shapira, C.K. Johnson, K. Saylor, E.M. Rubin, K. Chandran, W.I. Lipkin, J.A.K. Mazet, The discovery of Bombali virus adds further support for bats as hosts of ebolaviruses, *Nature Microbiology* 3 (2018) 1084–1089.
- [2] R.T. Emond, B. Evans, E.T. Bowen, G. Lloyd, A case of Ebola virus infection, *Br. Med. J.* 6086 (1977) 541–544.
- [3] World Health Organization. <https://www.who.int/>.
- [4] E.D. Laing, I.H. Mendenhall, M. Linster, D.H.W. Low, Y. Chen, L. Yan, S.L. Sterling, S. Borthwick, E.S. Neves, J.S.L. Lim, M. Skiles, B.P.Y.-H. Lee, L.-F. Wang, C.C. Broder, G.J.D. Smith, Serologic evidence of fruit bat exposure to filoviruses, Singapore, 2011–2016, *Emerg. Infect. Dis.* 24 (2018) 114–117.
- [5] J. Yuan, Y. Zhang, J. Li, Y. Zhang, L.F. Wang, Z. Shi, Serological evidence of ebolavirus infection in bats, China, *Virol. J.* 9 (2012) 236.
- [6] T. Hoenen, A. Groseth, H. Feldmann, Therapeutic strategies to target the Ebola virus life cycle, *Nat. Rev. Microbiol.* 17 (2019) 593–606.
- [7] D.S. Yu, T.H. Weng, X.X. Wu, F.X.C. Wang, X.Y. Lu, H.B. Wu, L.-J. Li, H.-P. Yao, The lifecycle of the Ebola virus in host cells, *Oncotarget* 8 (33) (2017) 55750–55759.
- [8] J.A. Simmons, R.S. D'Souza, M. Ruas, A. Galione, J.E. Casanova, J.M. White, Ebolavirus glycoprotein directs fusion through NPC1+ endolysosomes, *J. Virol.* 90 (2015) 605–610.
- [9] M. Anantpadma, J. Kouznetsova, H. Wang, R. Huang, A. Kolokoltsov, R. Guha, A.R. Lindstrom, O. Shtanko, A. Simeonov, D.J. Maloney, W. Maury, D.J. LaCount, A. Jadhav Davey, A. R. Large-scale screening and identification of novel Ebola virus and Marburg virus entry inhibitors, *Antimicrob. Agents Chemother.* 60 (2016) 4471–4481.
- [10] W.A. van der Linden, C.J. Schulze, A.S. Herbert, T.B. Krause, A.A. Wirchnianski, J.M. Dye, K. Chandran, M. Bogyo, Cysteine cathepsin inhibitors as anti-ebola agents, *ACS Infect. Dis.* 2 (3) (2016) 173–179, <https://doi.org/10.1021/acscinfed.5b00130>.
- [11] Y. Sakurai, A.A. Kolokoltsov, C.-C. Chen, M.W. Tidwell, W.E. Bauta, N. Klugbauer, C. Grimm, C. Wahl-Schott, B. Martin, D. Robert, Two pore channels control Ebolavirus host cell entry and are drug targets for disease treatment, *Science* 347 (6225) (2015) 995–998, <https://doi.org/10.1126/science.1258758>.
- [12] J. Ren, Y. Zhao, E.E. Fry, D.I. Stuart, Target identification and mode of action of four chemically divergent drugs against Ebolavirus infection, *J. Med. Chem.* 61 (2018) 724–733.
- [13] A.S. Sokolova, O.I. Yarovaya, D.V. Korzhagina, V.V. Zarubaev, T.S. Tretiak, P.M. Anfimov, O.I. Kiselev, N.F. Salakhutdinov, Camphor-based symmetric diimines as inhibitors of influenza virus reproduction, *Bioorg. Med. Chem.* 22 (2014) 2141–2148.
- [14] A.S. Sokolova, O.I. Yarovaya, M.D. Semenova, A.A. Shtro, I.R. Orshanskaya, V.V. Zarubaev, N.F. Salakhutdinov, Synthesis and in vitro study of novel borneol derivatives as potent inhibitors of the influenza A virus, *Med. Chem. Commun.* 8 (2017) 960–963.
- [15] A.S. Sokolova, O.I. Yarovaya, D.S. Baev, A.V. Shernyukov, A. Shtro, V.V. Zarubaev, N.F. Salakhutdinov, Aliphatic and alicyclic camphor imines as effective inhibitors of influenza virus H1N1, *Eur. J. Med. Chem.* 127 (2017) 661–670.
- [16] A.S. Sokolova, O.I. Yarovaya, A.V. Shernyukov, Y.V. Gatilov, Y.V. Razumova, V.V. Zarubaev, T.S. Tretiak, O.I. Kiselev, N.F. Salakhutdinov, Discovery of a new class of antiviral compounds: camphor imine derivatives, *Eur. J. Med. Chem.* 105 (2015) 263–273.
- [17] V.V. Zarubaev, A.V. Garshinina, T.S. Tretiak, V.A. Fedorova, A.A. Shtro, A.S. Sokolova, O.I. Yarovaya, N.F. Salakhutdinov, Broad range of inhibiting action of novel camphor-based compound with anti-hemagglutinin activity against influenza viruses in vitro and in vivo, *Antivir. Res.* 120 (2015) 126–133.
- [18] F.A. Rey, Sh.-M. Lok, Common features of enveloped viruses and implications for immunogen design for next-generation vaccines, *Cell* 172 (2018) 1319–1334.
- [19] A.A. Kononova, A.S. Sokolova, S.V. Cheresiz, O.I. Yarovaya, R.A. Nikitina, A.A. Chepurnov, A.G. Pokrovsky, N.F. Salakhutdinov, N-Heterocyclic borneol derivatives as inhibitors of Marburg virus glycoprotein-mediated VSIV pseudotype entry, *Med. Chem. Commun.* 8 (2017) 2233–2237.
- [20] A.S. Sokolova, O.I. Yarovaya, N.I. Bormotov, L.N. Shishkina, N.F. Salakhutdinov, Discovery of a new class of inhibitors of Vaccinia virus based on (-)-borneol from *Abies sibirica* and (+)-camphor, *Chem. Biodivers.* 15 (2018), e1800153.
- [21] L.M. Johansen, L.E. DeWald, C.J. Shoemaker, B.G. Hoffstrom, C.M. Lear-Rooney, A. Stossel, E. Nelson, S.E. Delos, J.A. Simmons, J.M. Grenier, L.T. Pierce, H. Pajouhesh, J. Lehár, L.E. Hensley, P.J. Glass, J.M. White, G.G. Olinger, A screen of approved drugs and molecular probes identifies therapeutics with anti-Ebola virus activity, *Sci. Transl. Med.* 7 (2015), 290ra89.
- [22] C.A. Lipinski, F. Lombardo, B.W. Dominy, Feeney, P.J. Experimental and computational approaches to estimate solubility and permeability in drug discovery and development settings, *Adv. Drug Deliv. Rev.* 64 (2012) 4–17.
- [23] A.K. Ghose, V.N. Viswanadhan, J.J. Wendoloski, A knowledge-based approach in designing combinatorial or medicinal chemistry libraries for drug discovery. 1. A qualitative and quantitative characterization of known drug databases, *J. Combin. Chem.* 1 (1999) 55–68.
- [24] M.-H. Wang, L.-Y. Chen, An efficient FeCl<sub>3</sub>-mediated approach for reduction of ketones through N-heterocyclic carbene boranes, *Tetrahedron Lett.* 58 (2017) 732–735.
- [25] E. Harder, W. Damm, J. Maple, C. Wu, M. Reboul, J.Y. Xiang, L. Wang, D. Lupyan, M.K. Dahlgren, J.L. Knight, J.W. Kaus, D.S. Cerutti, G. Krilov, W.L. Jorgensen, R. Abel, R.A. Friesner, OPLS3: a force field providing broad coverage of drug-like small molecules and proteins, *J. Chem. Theor. Comput.* 12 (2016) 281–296.
- [26] R.A. Friesner, R.B. Murphy, M.P. Repasky, L.L. Frye, J.R. Greenwood, T.A. Halgren, P.C. Sanschagrin, D.T. Mainz, Extra precision Glide: docking and scoring incorporating a model of hydrophobic enclosure for Protein–Ligand complexes, *J. Med. Chem.* 49 (2006) 6177–6196.
- [27] M.A. Whitt, Generation of VSV pseudotypes using recombinant ΔG-VSV for studies on virus entry, identification of entry inhibitors, and immune responses to vaccines, *J. Virol Methods* 169 (2010) 365–374.
- [28] D.M. Morgan, Tetrazolium (MTT) assay for cellular viability and activity, *Methods Mol. Biol.* 79 (1998) 179–183.